UNIVERSITÀ
DEGLI STUDI
DI PADOVA

UNIVERSITA' DEGLI STUDI DI PADOVA

DIPARTIMENTO DI NEUROSCIENZE – DNS

Ph.D. COURSE IN NEUROSCIENCE

XXXIV Cycle

Exploring multiple sclerosis brain microstructural damage through T1w/T2w-ratio: a multicenter study

Coordinator: Ch.mo Prof. Antonino Vallesi

Supervisor: Ch.mo Prof. Paolo Gallo

Ph.D. candidate: Monica Margoni

To my parents

ABSTRACT

Background. The T1-weighted (w)/T2w-ratio has been proposed as a clinically feasible method to investigate white matter (WM) and gray matter (GM) integrity in multiple sclerosis (MS). However, its clinical relevance and suitability in a multicenter setting still need to be fully explored.

Objective. To evaluate WM and GM T1w/T2w-ratio in a large multicenter cohort of healthy controls (HC) and MS patients, and its association with clinical disability.

Methods. Brain T2w and T1w scans were identified retrospectively at 7 European sites from 434 MS patients (57 clinically isolated syndrome, 196 relapsing-remitting [RR], 106 secondary progressive [SP], 75 primary progressive [PP]) and 270 HC. T1w/T2w-ratio maps were obtained after calibrating signal intensities to eyes and temporal muscle. Sex- and site-adjusted lifespan trajectories of T1w/T2w-ratio were estimated in different brain structures of HC using linear mixed models. Then, sex-, age- and site-specific T1w/T2w-ratio z-scores were derived in MS patients and compared among different clinical phenotypes and levels of disability. The associations with clinical and MRI variables were investigated.

Results. In HC, T1w/T2w-ratio increased with age until 50-60 years both in WM and GM. Compared to HC, T1w/T2w-ratio was significantly lower in WM lesions of all MS phenotypes, and in normal-appearing (NA) WM and cortex of RRMS and SPMS patients ($p \leq 0.026$), but it was significantly higher in the striatum and pallidum of RRMS, SPMS and PPMS patients ($p \leq 0.042$). Furthermore, compared to HC, T1w/T2w-ratio was significantly lower in WM lesions and NAWM in relapse-onset MS patients with mild levels of disability (Expanded Disability Status Scale [EDSS]<3.0) and in the cortex in relapse-onset MS patients with EDSS≥3.0 ($p \leq 0.023$). Conversely, T1w/T2w-ratio was significantly higher in the striatum and pallidum in relapse-onset MS patients starting at EDSS≥4.0 ($p \leq 0.005$). In PPMS, T1w/T2w-ratio was significantly higher in the striatum and pallidum beyond EDSS≥6.0 ($p \leq 0.001$). In MS, longer disease duration, higher EDSS, higher brain T2-hyperintense lesion volume, and lower normalized brain volume were associated with lower T1w/T2w-ratio in WM lesions and cortex and a higher T1w/T2w-ratio in the striatum and pallidum (β from -1.168 to 0.286, $p \leq 0.040$).

Conclusions. Compared to HC, heterogeneous T1w/T2w-ratio abnormalities were detected in specific brain compartments according to MS clinical phenotypes and

disability. Various pathological substrates, including demyelination, inflammation, neurodegeneration, and iron accumulation may explain alterations of this index and their clinical relevance.

RIASSUNTO

Introduzione. Il rapporto tra le sequenze pesate in T1 (T1w) e T2 (T2w), ossia il T1w/T2w, è stato proposto come un metodo applicabile clinicamente per studiare l'integrità della sostanza bianca e della sostanza grigia nella sclerosi multipla (SM). Tuttavia, la sua rilevanza clinica e l'applicabilità in un contesto multicentrico devono ancora essere completamente indagate.

Obiettivi. Quantificare il rapporto T1w/T2w nella sostanza bianca e nella sostanza grigia in un'ampia coorte multicentrica di pazienti affetti da SM e controlli sani, e la sua associazione con la disabilità clinica.

Metodi. Le sequenze T1w e T2w dell'encefalo di 434 pazienti con SM (57 con sindrome clinicamente isolata, 196 recidivante-remittente [RR], 106 secondariamente progressiva [SP], 75 primariamente progressiva [PP]) e 270 controlli sani sono state identificate retrospettivamente in 7 centri europei. Le mappe del rapporto T1w/T2w sono state ottenute dopo aver calibrato le intensità del segnale utilizzando gli occhi ed il muscolo temporale. Nei controlli sani, l'andamento del rapporto T1w/T2w con l'età è stato stimato in diverse strutture cerebrali aggiustando per sesso e centro, utilizzando modelli lineari misti. Sono stati quindi derivati i punteggi z del rapporto T1w/T2w specifici per età, sesso e centro nei pazienti con SM e confrontati tra i diversi fenotipi clinici e livelli di disabilità. Infine, sono state studiate le associazioni con le variabili cliniche e di risonanza magnetica.

Risultati. Nei controlli sani, il rapporto T1w/T2w aumentava con l'età fino ai 50-60 anni sia nella sostanza bianca che nella sostanza grigia. Rispetto ai controlli sani, il rapporto T1w/T2w risultava significativamente più basso nelle lesioni della sostanza bianca di tutti i fenotipi clinici della SM e nella sostanza bianca apparentemente normale e nella corteccia dei pazienti con SMRR e SMSP ($p \leq 0.026$). Al contrario, il rapporto T1w/T2w era significativamente più alto nello striato e nel pallido dei pazienti con SMRR, SMSP e SMPP rispetto ai controlli sani ($p \leq 0.042$). Inoltre, rispetto ai controlli sani, il rapporto T1w/T2w era significativamente più basso nelle lesioni della sostanza bianca e della sostanza bianca apparentemente normale nei pazienti con esordio a ricadute e basso livello di disabilità (Expanded Disability Status Scale [EDSS] <3.0) e nella corteccia dei pazienti con esordio a ricadute ed EDSS≥3.0 ($p \leq 0.023$). Al contrario, il rapporto T1w/T2w era significativamente più alto nello striato e nel pallido nei pazienti con

esordio a ricadute ed EDSS≥4.0 ($p \leq 0.005$). Nei pazienti con SMPP, il rapporto T1w/T2w era significativamente più alto nello striato e nel pallido solo con EDSS≥6.0 ($p \leq 0.001$). Nei pazienti con SM, una durata di malattia più lunga, un EDSS ed un volume di lesioni della sostanza bianca più elevati, ed un volume cerebrale normalizzato più basso, risultavano essere associati ad un rapporto T1w/T2w più basso nelle lesioni della sostanza bianca e nella corteccia, e ad un rapporto T1w/T2w più elevato nello striato e nel pallido (β da -1.168 a 0.286, $p \leq 0.040$).

Conclusioni. Rispetto ai controlli sani, nei pazienti affetti da SM abbiamo osservato alterazioni eterogenee del rapporto T1w/T2w nelle diverse regioni cerebrali ed in base al fenotipo clinico ed al grado di disabilità. Vari substrati patologici, tra cui la demielinizzazione, l'infiammazione, la neurodegenerazione e l'accumulo di ferro, possono spiegare le alterazioni di questo indice e la loro rilevanza clinica.

1. INTRODUCTION

Multiple sclerosis (MS) is a chronic inflammatory, demyelinating, and neurodegenerative disease of the central nervous system (CNS).[1]

MS typically affects young adults, with a higher prevalence in females than males and with an onset between 20 and 40 years of age, although up to 10% of patients experience their first attack during childhood or adolescence. This disorder is typically considered a multifactorial disease that is caused by a complex interaction among several environmental and genetic factors.

Pathologically, MS is characterized by the accumulation of focal inflammatory demyelinating lesions affecting both the white matter (WM) and the gray matter (GM) of the brain and spinal cord, together with oligodendrocyte loss, reactive gliosis and neuro-axonal degeneration. These pathological processes determine heterogeneous clinical manifestations, course and disability progression over time. In the majority of patients, reversible episodes of neurological deficits, usually lasting days or weeks, distinguish the initial phases of the disease (i.e., relapsing-remitting MS [RRMS],[2] whereas a minority of patients (~10-15%) have a progressive course from disease onset (i.e., primary progressive MS [PPMS]). Over time, the development and progression of irreversible clinical deficits become prominent and affect profoundly MS patients' daily activity and their quality of life.

The diagnosis of MS is based on clinical findings and paraclinical tools, requires the exclusion of alternative diagnoses,[3] and involves the demonstration of a pathological process affecting at least two different CNS regions (i.e., dissemination in space [DIS]) which has occurred at different times (i.e., dissemination in time [DIT]).[4] Although the diagnosis can be made on the basis of clinical criteria alone, magnetic resonance imaging (MRI) can support, supplement, or even replace some clinical criteria, thus allowing an earlier diagnosis of MS.

Due to its high sensitivity in revealing disease-related abnormalities, MRI has significantly improved the understanding of MS pathophysiology and the management of MS patients, not only during their diagnostic work-up, but also for monitoring the disease course and treatment response, contributing to influencing treatment decisions.

1.1. Epidemiology

MS is associated with a high societal economic burden, which has increased over time.[5] Typically, the mean age of onset ranges from 20-40 years, even though up to 10% of MS patients experience their first attack before 18 years of age,[6] and from 4% to 10% after 60 years of age.[7] Conversely, in MS patients with a progressive course from onset, the disease typically starts later, generally from the fifth decade of age.

Approximately ~2.3 million people have MS worldwide,[5] however, the prevalence and incidence of MS are highly variable with both environmental and genetic factors playing a role (Figure 1).

The importance of the environment is demonstrated by the peculiar geographic distribution of the disease, with a trend towards a higher prevalence with increasing latitudes.[5, 8] Indeed, the highest prevalence is found in northern Europe and north America (typically ~1 case per 1.000 individuals, but up to 1 case per 400 individuals in some countries with higher latitudes), medium prevalence is reported in southern Europe and southern United States of America (USA) (5-30 per 100.000); while Asia, Africa and South America have a very low burden of disease (<5 per 100.000).[8] These geographical variations may in part be attributed to genetic predisposition. However, the role of acquired, environmental factors have been highlighted by several studies showing that the risk of MS correlates with the country of residence during childhood and that migration from high-risk to low-risk areas in early life leads to a decreased susceptibility.

Interestingly, the prevalence of MS has increased over time since the 1950s,[5, 8] and this is more evident in women. This finding might be attributed to improved access to medical facilities, better diagnostic accuracy and increased life expectancy owing to improved management. However, these cannot explain changes in female preponderance. Of note, although a diffuse gender difference with females being more frequently affected than males has been consistently demonstrated, the female-to-male ratio has increased from 2:1 in 1950s up to ~3:1 in 2010s.[8, 9] This might suggest the role of environmental risk factors mainly affecting women (i.e., occupation, increased cigarette smoking, obesity, birth control, and later childbirth) as contributor of such an increase of female MS preponderance.[8, 9]

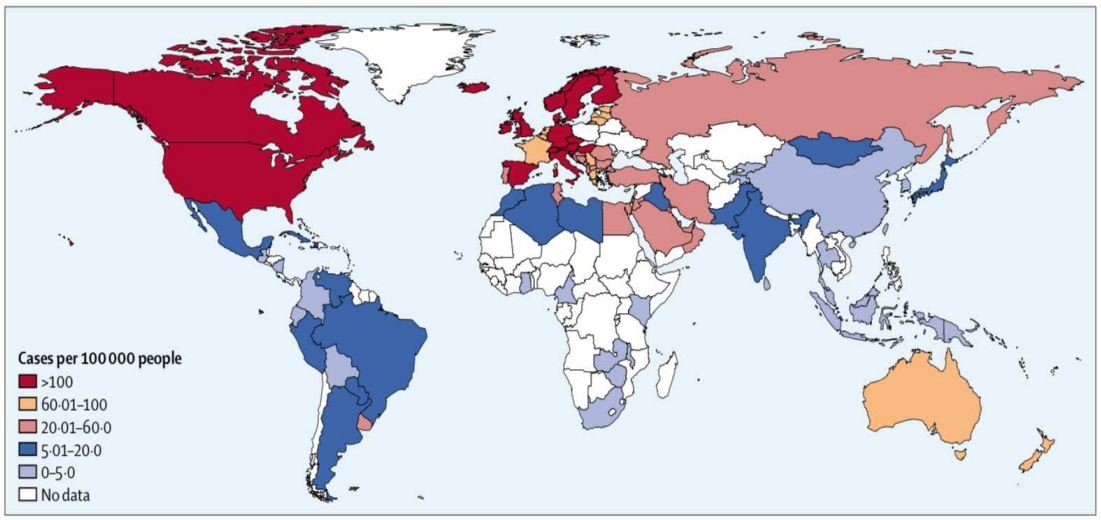

Figure 1. Global prevalence of multiple sclerosis. *Reproduced from Atlas of MS 2013, MS International Federation*

1.2. Pathogenesis of multiple sclerosis

1.2.1. Environmental risk factors

Environmental risk factors such as vitamin D deficiency (related to reduced exposure to sunlight and decreased natural production from sun exposure in ethnic groups with dark skin), obesity in early life, diet and cigarette smoking are known to play a part in development of MS.[10] Their identification might contribute not only to better understand the pathological substrates of the disease but also to prevent the onset and to limit the progression of the disease, since some factors are modifiable.[11]

Due to the immune-mediated pathogenesis of MS, it has been hypothesized that some infections could trigger disease onset. Many pathogens have been proposed to play a role in MS, and Epstein Barr Virus (EBV) is the most consistently associated.[10, 12] An EBV infection in adolescence or early adulthood, and a history of infectious mononucleosis have been associated with an increased MS risk. A molecular mimicry between EBV and myelin antigens is likely to represent the pathological mechanism linking EBV infection and MS. However, the definite demonstration of causality is still lacking.

Sun exposure, and mainly exposure to ultraviolet B radiation, is the major determinant of vitamin D levels, that tend to decrease with increasing latitudes and thus could contribute to the 'latitude effect' found in MS. Recently an immunomodulatory role (i.e., reduction of inflammatory activity) of the active form of vitamin D, 1,25-

dihydroxycholecalciferol has been demonstrated.[10, 13, 14] In addition, recent findings showed that low vitamin D intake or serum vitamin D status are associated with increased risk of developing MS. Furthermore, in MS patients an association between low vitamin D levels and clinical and MRI activity has been observed, suggesting a beneficial effect of vitamin D supplementation throughout the course of the disease.[10, 14]

Smoking has been consistently demonstrated as a risk factor for MS.[10] The risk of MS is positively correlated with the amount of smoking, both active and passive.[10] Smoking is also associated with an increased risk of early and more severe disability progression and to a faster conversion to secondary progressive (SP) MS.[10, 15] Possible mechanisms for this association include a chronic inflammatory activity in the lung, with a higher activation of the immune system, but also a direct toxic effect of some smoke components with detrimental effects for several cells, including neurons and oligodendrocytes.

Recent studies have also suggested that the gut microbiota, the combination of bacteria that colonize the human intestine, could modulate the activity of innate and adaptive immunity, thus contributing to disease pathogenesis.[16]

1.2.2. Genetics

Several genetic factors may play a role in MS susceptibility and disease evolution. Pivotal epidemiological studies showed the presence of familial aggregation in MS patients, thus suggesting the role of genetic risk factors. In particular, relatives of people with MS are more likely to develop the disease than the general population, with the risk inversely associated with the degree of relatedness. The prevalence of familial MS is ~13% for all MS phenotypes.[17] The risk of recurrence within families increases with percentage of genetic sharing, ranging from 35% in monozygotic twins to 3% in siblings and first-degree relatives.[18] However, the heritability of MS is polygenic and involves polymorphisms in several genes, each of which contributes with a small increase in disease risk.

The first genetic factor found is located in the HLA class I region on chromosome 6p21.3.[10, 18] The HLA cluster encompasses more than 200 genes within 4.5 megabases, with important roles in several immunological processes.[10, 18] Specifically, the strongest

association pointed to the so called '*HLA-DR15* haplotype', including *HLA-DRB1*1501* and *HLA-DQB1*0602,* that conveys the highest risk for MS.[10, 18]

Thanks to the advance in genotyping technologies that allowed obtaining whole genome information on thousands of individuals, in the last few years the knowledge of MS genetic architecture has significantly improved. Genome-wide association studies have identified over 200 genetic risk variants for MS. Each variant has a small effect on the risk of disease, and different combinations of these variants likely contribute to genetic susceptibility in different patients.[19] Most of these polymorphisms encode molecules involved in the immune system (such as polymorphisms in interleukin 2 receptor [*IL2R*] and interleukin 7 receptor [*IL7R*]) and are associated with a higher risk for other systemic dysimmune disorders. Others are involved in other biological processes, such as vitamin D metabolism, suggesting that environmental risk factors are likely to interact with MS susceptibility genes to influence the risk to develop MS.[10]

1.2.3. From immune to responses to pathology

The pathological hallmark of MS is the formation of focal plaques, characterized by areas of demyelination, in the CNS. Such lesions are typically located around post-capillary venules and in the acute phase are associated with the breakdown of the blood-brain barrier (BBB). This promotes the migration of activated innate (i.e., macrophages) and adaptive immune cells (T and B cells) into the CNS, thus causing inflammation and demyelination, that are followed by oligodendrocyte loss, reactive gliosis and neuro-axonal degeneration.[20]

MS plaques occur both in the WM and GM and are typically disseminated throughout the CNS, including the brain, optic nerves and spinal cord.[21-23]

Active lesions are frequent in earlier phases of the disease, whereas their prevalence becomes lower in the later course of the disease. These lesions are infiltrated by lymphocytes (mainly $CD8^+$ T cells and $CD20^+$ B cells), activated microglia and macrophages containing myelin debris, and large reactive, sometimes multinucleated, astrocytes.[24, 25]

Conversely, progressive (P) MS patients are mainly characterized by inactive lesions, that are sharply circumscribed, with reduced axonal and cellular densities, with a well-defined limit of demyelination, reactive gliosis and a variable degree of activated microglia only

in the periplaque WM.[24-28] Nevertheless, inflammation is present also in PMS patients. Some of preexisting plaques, defined as 'chronic active' or 'mixed inactive/active' comprised up to 57% of all lesions in patients with PMS.[29] These are characterized by iron-laden microglia/macrophages at their edge, diminishing towards their inactive center,[24, 29, 30] and by a smouldering inflammation promoting a slow rate of ongoing demyelination and axonal transection and a progressive, expansion of their size.[31]
A mild degree of demyelination, macrophage and lymphocyte infiltration, activated microglia and neurodegenerative phenomena, including astrocyte gliosis and axonal damage and loss, are also present in the absence of foCal demyelination, in the so-called normal-appearing (NA) WM.[27, 32] These abnormalities occur from the earliest phases of the disease and seem to occur at least partially independently from the accumulation of focal lesions.[21]

A diffuse GM involvement also occurs from the earliest phases of the disease and becomes more and more severe in PMS patients.[33, 34]

Reparative processes have been also described in MS. For instance, remyelination may occur in MS,[35-37] thus representing a promising target for future treatments.[38] Such a phenomenon gives rise to the so-called 'shadow' plaques, that are characterized by global or patchy remyelination, a sharply demarcation from the surrounding WM, and axons showing thin myelin sheats and shortened internodes.[35, 36, 39, 40] The extent of remyelination is heterogeneous, is more frequent in GM than in WM lesions, and depends on several factors, including patients' age, disease duration, lesion location, the presence of oligodendrocyte progenitors, and the integrity of axonal function.[41] While a significant remyelination is frequently encountered during the earlier phases of MS and in younger subjects, it is sparser or absent in PMS.[42]

The immunopathophysiology of MS showed a significant evolution during the last years (Figure 2).[30]

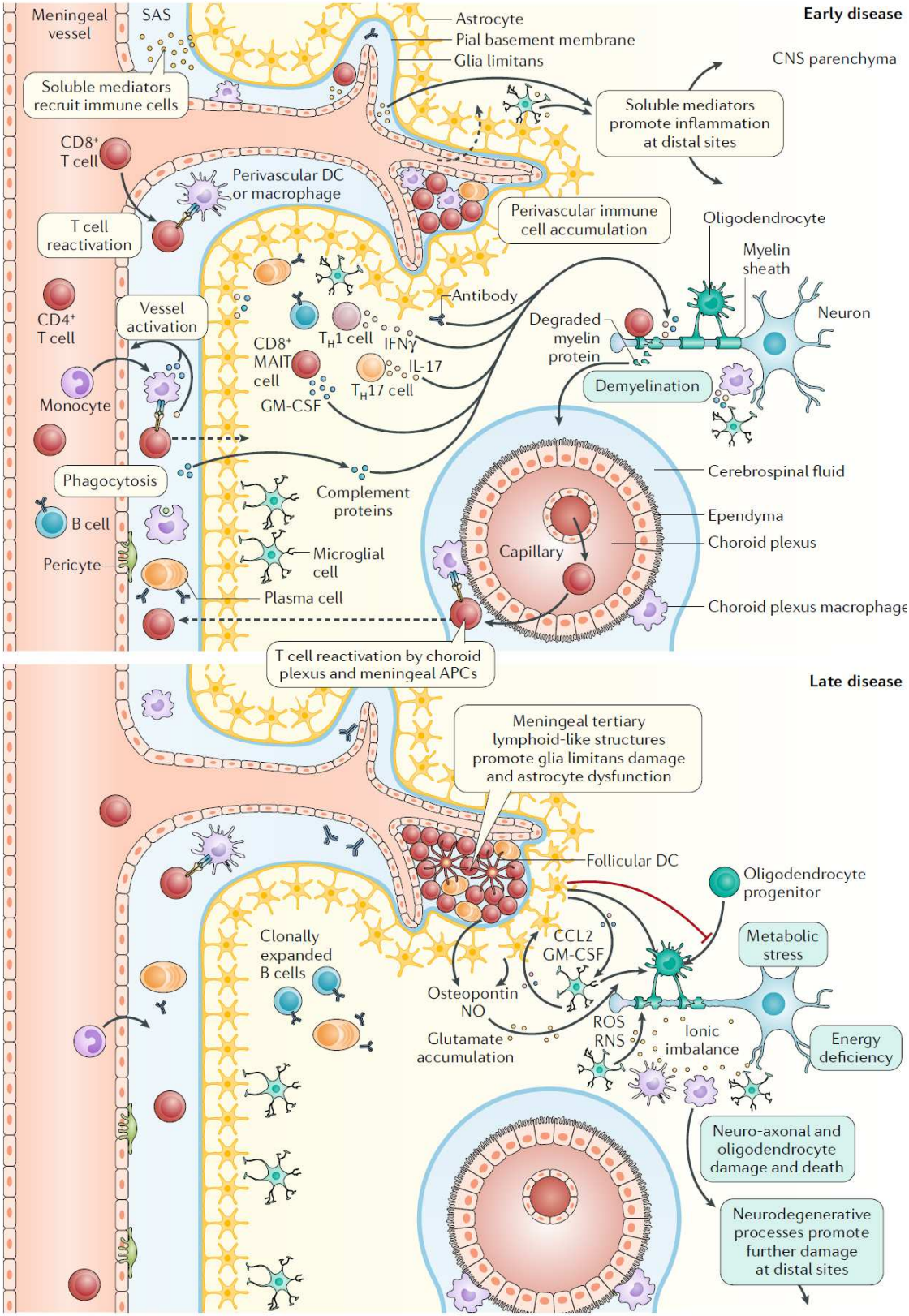

Figure 2. Immunopathophysiology of MS. From Filippi et al.[1]

Although the initial antigenic targets and mechanisms that trigger the immune response are still unknown, historically, the aberrant activation of effector T cells (CD4+ and CD8+) has been considered the key factor of MS inflammatory activity.[30] T cell activation, possibly promoted by a molecular mimicry with antigens of infectious agents, is then sustained by an imbalance in immune regulatory activity and by a progressive T cell activation to additional CNS antigens triggered as a consequence of CNS injury ('epitope spreading') which may contribute to the propagation of chronic immune responses.[30]

Although typically considered a 'T cell-mediated' disease, recent studies suggest that MS inflammatory activity includes relevant bidirectional interactions between innate immunity (including myeloid cells) and adaptive immunity (T and B cells), as well as resident CNS cells, such as microglia and astrocytes.[30, 43]

Recent evidence coming from the results of selective B cell targeting therapy clearly changed the immunopathophysiology framework of MS.[30, 43] While the original hypothesis for B cells role in MS was based on the abnormally production of antibodies, it is now clear that other antibody-independent functions are relevant.[30, 43] These include an increased production of pro-inflammatory cytokines, a deficient capacity to produce regulatory cytokines and B cell contribution as antigen-presenting cells for T lymphocytes.[30, 43]

The interplay between peripheral immune cells and CNS-resident cells may promote the setting of a pro-inflammatory environment, with the secretion of a wide range of pro-inflammatory mediators that can increase BBB permeability, thus further promoting the recruitment and the activation of inflammatory cells into the CNS and leading to inflammation, demyelination and neuro-axonal damage.[30, 43]

Furthermore, growing body of evidence suggests that different types of inflammatory processes can occur in MS. Beside peripheral inflammatory mechanisms, the role of CNS-compartmentalized inflammation (i.e., inflammation localized with the CNS or in the meninges) has been suggested to strongly contribute to CNS injury, although it is likely to be poorly targeted by currently available treatments.[41, 44, 45]

1.3. Clinical features

1.3.1. Clinical manifestations

The clinical symptoms of MS are heterogeneous and depend on the topography of focal and diffuse CNS damage.

Typically, in ~85% of patients, MS onset is characterized by a first acute episode of neurological dysfunction (defined as clinically isolated syndrome [CIS]) that can affect the spinal cord, the optic nerve, the cerebellum or the brainstem, or the cerebral hemispheres.[46, 47] This consists of a reversible episode of neurological deficits, known as relapse,[48-50] lasting at least 24 hours, reaching a peak of severity within 2-3 weeks and being followed by spontaneous remission with variable degrees of recovery after a few weeks. During disease course, further relapses may occur, developing at irregular intervals, being followed by spontaneous remission with partial or complete recovery and characterizing the RR form of the disease.

Optic neuritis is the first neurological episode in ~25% of patients and can occur in up to 70% of MS patients along their disease course.[51-53] Optic nerve involvement is characterized by a partial or total visual loss in one eye with a central scotoma and dyschromatopsia. Visual disturbances are often associated with orbit pain that is worsened by eye movement.[51-53] If inflammation involves the optic disc, the optic nerve head may show inflammation (papillitis) and disc oedema. Optic nerve involvement may be also subclinical and can be demonstrated by afferent pupillary defect or abnormalities at paraclinical tests (visual evoked potentials [VEPs], optical coherence tomography [OCT] or MRI).

Somatosensory symptoms represent the clinical onset of up to 43% of MS patients, typically due to brainstem or spinal cord involvement.[54] These include paresthesia (numbness, tingling and/or pins-and-needles tightness, coldness, or swelling of the limbs or trunk), Lhermitte sign (a transient electric sensation running through the back and into le limbs promoted by neck flexion), impairment of vibration and joint position sensation and reduced pain and light touch perception. A transient worsening of these symptoms can occur with increased temperature (Uhthoff phenomenon).

Motor manifestations are the first symptoms in 30-40% of patients, affect the majority of MS patients during disease course and occur due to brainstem, spinal cord or hemispheric involvement.[55] These include pyramidal signs (Babinski sign, brisk reflexes, clonus, etc.), spasticity, and paresis.

Impairment in ocular movements (i.e., nystagmus, oscillopsia and diplopia), ataxia and gait imbalance, dysmetria, complex movements decomposition, slurred speech and dysphagia are typical manifestations due to brainstem and cerebellar involvement and can affect up to 70% of MS patients.[55]

Sphincter and sexual dysfunctions are also common, especially in PMS and in those with motor disability.[56] They include bladder dysfunction such as urinary urgency hesitancy, frequency and urge incontinence.[56] Constipation is more common than fecal incontinence, while men with MS often suffer from erectile dysfunction and impotence.

Up to 40-70% of patients with MS have cognitive impairment, starting in the earliest phases of the disease and being more pronounced in PMS.[57] Cognitive deficits include impairment in information processing speed, episodic memory, attention, efficiency of information processing and executive functions.[57]

Fatigue is experienced in up to 75-95% of MS patients. This manifestation can be associated with recent disease activity; however, it can persist after the attack and can be independent from relapses or the severity of clinical disability. Neurophysiological and imaging data have suggested that a dysfunction of cortico-subcortical circuits, mainly affecting fronto-parietal regions and the basal ganglia could contribute to MS-related fatigue.[58]

Affective disturbance occurs in up to two-thirds of patients, of which, depression is the most common manifestation.[59]

Finally, pain is reported in up to 43% of MS patients, and includes trigeminal neuralgia, dysesthetic pain, back pain, visceral pain and painful tonic spasms.[60]

1.3.2. Clinical phenotypes

In 1996, the National MS Society Advisory Committee on Clinical Trials in MS [61] defined four MS clinical courses: RRMS, SPMS, PPMS, and progressive-relapsing (PR) MS (Figure 3).

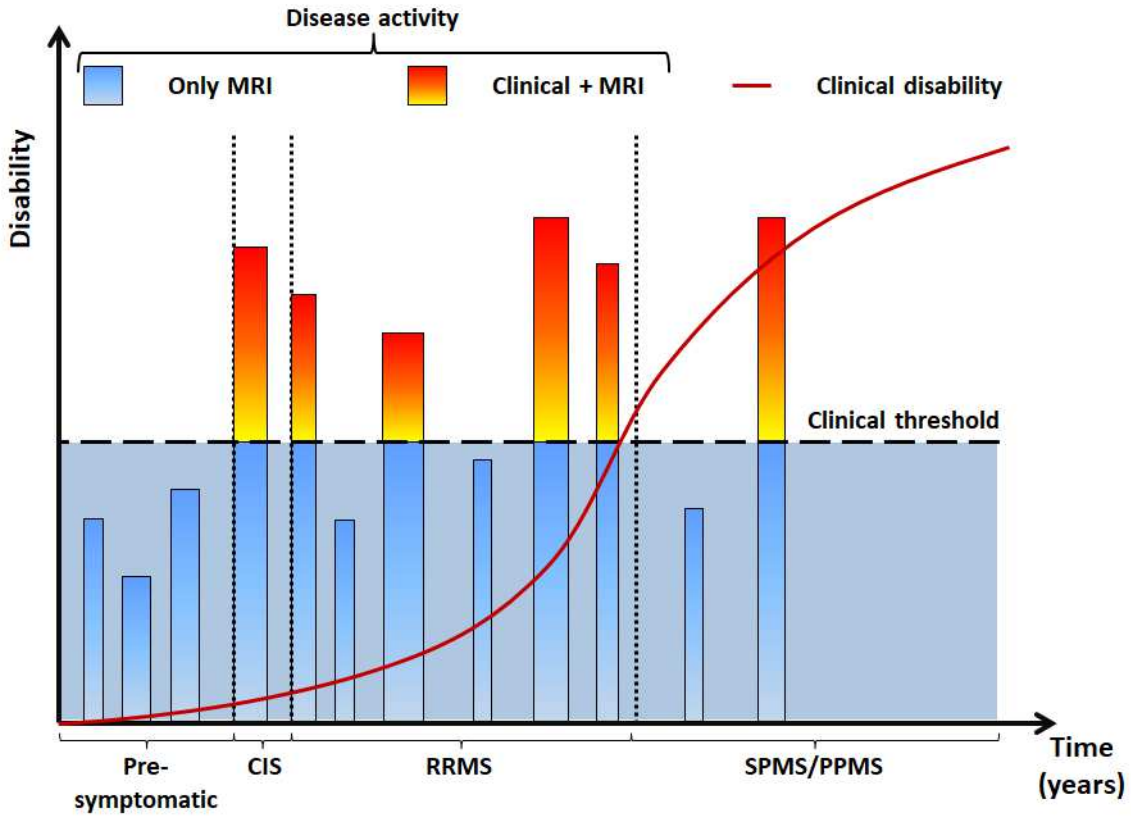

Figure 3. Clinical courses of MS.

RRMS is the most common type (approximately 85% of MS patients) and it is characterized by the occurrence of relapses, followed by spontaneous remission with variable degrees of recovery. In a significant proportion of RRMS patients, increasing with age and disease duration, the course of MS converts to SPMS, characterized by a progression of irreversible disability occurring independently from relapses.[61] SPMS conversion occurs at a rate of ~2–3% of patients per year.[62] About 10-15% of patients present a PP clinical phenotype, characterized by an insidious disease progression from the onset, resulting in gradual, progressive and unremitting accumulation of neurological deficits for more than one year, without preceding relapses and remissions.[4, 61] Finally, PR was an additional rare clinical course distinguished by progressive disease from the onset, with acute relapses, with or without full recovery and periods between relapses with continuing progression.[61]

An update of the definitions of these MS clinical phenotypes has been proposed in 2013, with the introduction of relevant changes (Figure 4).[2]

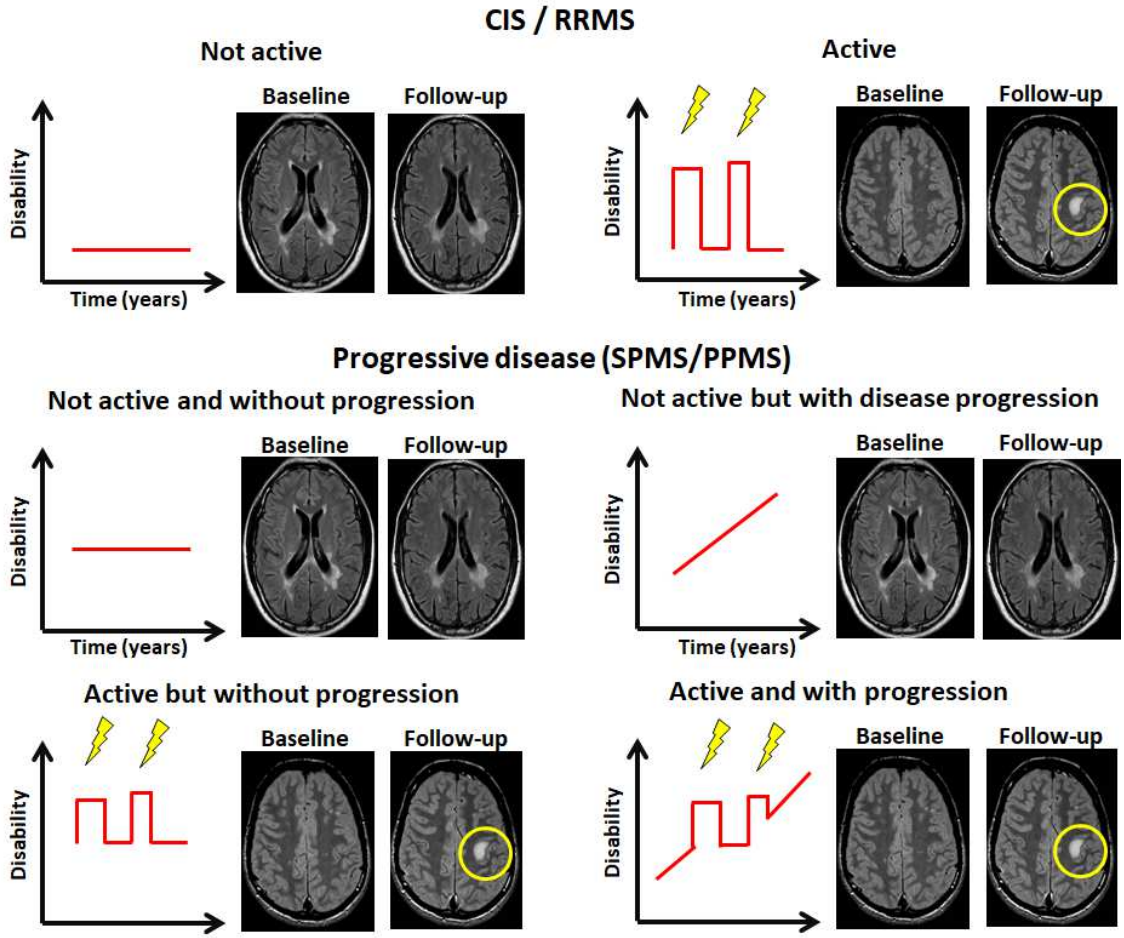

Figure 4. New definitions included in the 2013 revision of the MS clinical course.[2]

In the 2013 revision, CIS has been included in the spectrum of MS phenotypes to denote those patients with a first clinical presentation of the disease with characteristics of inflammatory demyelination that could be MS, but which has yet to fulfill the diagnostic criteria for MS.[2] Moreover, for each MS subtype, a classification of the disease as 'active' or 'not active', defined by clinical assessment of relapse occurrence or lesion activity detected by MRI has been added. Another important modification for the progressive stages has been the inclusion of whether disability has progressed over a given time period, thus identifying progressive patients with or without disability progression.[2]

1.4. Diagnosis

1.4.1. MRI

MRI is highly sensitive for detecting macroscopic abnormalities in the brain and spinal cord of MS patients. Abnormal MRI due to the presence of focal lesions is observed

in almost all patients with MS and in most patients with CIS. Specific features have been described to identify typical MS lesions,[63] that are defined as areas of focal hyperintensities on a T2-weighted (w) (T2, T2-fluid-attenuated inversion recovery [FLAIR] or similar) or a proton density (PD)-w sequence.

The administration of gadolinium (Gd)-based contrast agents and the acquisition of post-contrast T1w images allows to distinguish active from inactive lesions; signal enhancement, which underlies active lesions, occurs due to increased BBB permeability and corresponds to areas with ongoing inflammation. Lesions that persistently appear hypo intense on post-contrast T1w images (so-called 'black-holes') are associated with more severe tissue damage, suggestive of demyelination and axonal loss, compared with lesions that do not appear dark on such images. In the diagnostic criteria for MS, MRI has been used to confirm DIS or DIT for RRMS since 2001, and it has been included in the criteria for a diagnosis of PPMS.[4]

Recommendations aimed at optimizing and standardizing the use of MRI of the CNS in clinical practice have been given.[63-65]

1.4.2. Cerebrospinal fluid examination

Cerebrospinal fluid (CSF) findings supporting MS include a normal or mildly raised white cell count and protein, a raised IgG index ('Link index') and the presence of CSF-specific immunoglobulin G (IgG) oligoclonal bands (OCBs). CSF-specific OCBs were included in the latest revision of the MS diagnostic criteria[4] on the basis of their high prevalence in patients with MS (up to 88%)[66] and due to their role in predicting evolution to clinically definite MS.[67, 68]

1.4.3. Evoked potentials

Evoked-potentials, including sensory (VEPs, somatosensory and brainstem auditory) and motor evoked potentials, can assess functionally relevant pathways and can identify clinically silent lesions in the CNS determining prolonged latency and preserved waveform, which might be missed during standard routine clinical examination, thus supporting MS diagnosis.[69]

1.4.4. Diagnostic criteria

MS diagnosis requires the exclusion of alternative diagnoses,[3, 63, 70, 71] and the evaluation of clinical and paraclinical findings to demonstrate a pathological process affecting at least two different CNS regions (i.e., DIS) which have occurred at different times (i.e., DIT).[4]

The original Schumacher diagnostic criteria proposed in 1965 required evidence based on clinical examination alone for DIS and DIT.[72] Although they were developed before the introduction of MRI, these criteria still constitute a reference tool for some basic definitions, such as the concepts of DIS and DIT and the definition of a relapse. These criteria were subsequently modified in 1983 by Poser et al.,[73] who maintained the two clinical aspects as necessary components of the diagnosis, but included laboratory diagnostic tools such as CSF, evoked-potentials and neuroimaging.

Since 2001 up to the most recent revision proposed in 2017, MRI was formally included in the diagnostic algorithm for CIS patients with a suspicious of MS in the McDonald criteria.[4, 74-76]

1.4.5. Differential diagnosis

The range of diseases mimicking clinical manifestations and MRI features of MS is wide, and thus careful exclusion of other neurological disorders is essential in an MS diagnostic work-up.[3, 63, 70, 71]

Of note, the evidence-based criteria included in the 2017 revision of the McDonald diagnostic criteria have been demonstrated to be highly sensitive for distinguishing early relapsing forms of MS from monophasic CIS of CNS inflammation.[77] However, an inaccurate definition of the MRI diagnostic criteria and their improper application in the context of atypical clinical presentations increase the risk of misdiagnosis and consequently of inappropriate use of treatments.[63, 78, 79]

A careful definition of which clinical and imaging features are typical for MS (‘green flags’) and which are atypical or not suggestive of MS (‘red flags’) is crucial.[3, 63, 70, 71] The presence of ‘red flags’ should alert clinicians so that they reconsider the differential diagnosis in more detail.

Presentations that are similar to MS can occur in patients who have an infectious (i.e., meningitis, encephalitis and intracerebral abscess), neoplastic, hereditary (leukodystrophies, and Leber’s hereditary optic neuropathy), metabolic (i.e., Fabry's

disease, vitamin B12 and copper deficiency), vascular (i.e., cerebral autosomal dominant arteriopathy with subcortical infarcts and leukoencephalopathy [CADASIL], Susac's syndrome, primary angiitis of the CNS and dural arteriovenous fistula) or systemic immune-mediated disease (e.g., systemic lupus erythematosus, Behçet's disease, neurosarcoidosis and Sjögren's syndrome), non-MS idiopathic inflammatory demyelinating disease (mainly neuromyelitis optica spectrum disorder [NMOSD], anti-myelin oligodendrocyte glycoprotein [MOG] disease, and acute disseminated encephalomyelitis [ADEM]), or variants of MS (Balo's concentric sclerosis, Schilder's disease and Marburg MS).[3, 63, 70, 71]

1.4.6. Biomarkers and prognostic factors

In patients with CIS and early MS, several biomarkers and prognostic factors for the subsequent disease course (evolution to MS and accumulation of disability) have been identified, including environmental, genetic, clinical, laboratory and MRI features.[1]

In CIS patients, features associated with a higher risk of conversion to MS include environmental factors (low vitamin D level, smoking and EBV infections), genetic factors (*HLA-DRB1*1501*-positivity), a younger age, ethnic origin (non-white), sex (female), type of onset (optic neuritis and sensory involvement *vs* onset involving efferent pathways and monofocal *vs* multifocal onset), the presence of CSF OCBs and cognitive impairment. Several MRI findings at disease onset have been consistently seen among the strongest predictors of conversion to definite MS.[1]

The number of T2-hyperintense lesions at disease onset moderately contributes to predict the risk of long-term disability worsening.[80, 81] Change in T2-hyperintense lesion volume (LV) within the first years after disease onset, which is largely unpredictable, seems also to predict long-term physical disability worsening.[80] Lesion topography at disease onset particularly when asymptomatic lesions involve the infratentorial WM (mainly the brainstem),[82, 83] and the spinal cord, [84-86] also predicts disability worsening. For patients with CIS and brain MRI lesions, the chance of developing MS was greater than 80% during the subsequent 20 years.[80]

Prediction of the long-term clinical outcome (severity of disability, including death, and cognitive impairment) in MS is more difficult. In relapse-onset MS patients, predictors of poor outcome were gender (male), an older age at MS onset, the presence of CSF

OCBs, smoking, a higher relapse rate and a greater disability accumulation in the first 2-5 years of the disease and a shorter time to progress to SPMS.[1] Several imaging features, including T2-hyperintense lesion volume (LV) at baseline, the presence of infratentorial or spinal cord lesions and the formation of WM lesions in the first five years after clinical onset have also been associated with the accumulation of more severe disability over time.[1] A progressive disease from the onset and a faster rate of disability accumulation in the first 2 and 5 years are predictors of poor outcomes in PPMS.[1]

Several novel biomarkers are currently being investigated in an attempt to improve MS diagnosis and monitoring. Among them, neurofilaments (NfL) and OCT are the most promising for an application in the clinical setting.[87-90]

NfL are the major components of the axonal cytoskeleton, consisting of light, intermediate, and heavy chains that can be detected in the blood and CSF after axonal damage. Recent findings have demonstrated that higher NfL levels predict conversion to CIS in MS patients, are associated with a higher clinical and MRI disease activity, a greater disability, a higher probability to SP conversion, and a higher rate of brain atrophy.[87, 88]

OCT can generate high-resolution images of the retina in a non-invasive, rapid, and reproducible manner. OCT allows visualization of individual retinal layers and, in MS, the combined ganglion cell layer (GCL) and the retinal nerve fiber layer (RNFL) have been typically evaluated.

During acute optic neuritis, an initial thickening of RNFL can be observed due to acute inflammatory edema followed by atrophy within the subsequent 3 to 6 months.[89] Conversely, GCL has a faster onset of thinning without any acute-phase edema and GCL thickness might be an early indicator of neural changes following optic neuritis.[91]

Recent findings have shown associations of RNFL and GCL thinning or volume reduction with visual disability, overall clinical and MRI disease activity, disease course, disability progression and brain and spinal cord atrophy.[89, 90]

It is likely that also additional relevant biomarkers of disease activity and progression will be integrated in the future, including neuropsychological performances, serum NfL levels, patient-reported outcomes and quality of life measures.[92]

1.5. Conventional and advanced MRI

MRI has a high sensitivity in revealing macroscopic tissue abnormalities in MS patients. However, the association between conventional MRI findings and clinical disability remains modest in MS patients. This is likely due to the relative lack of specificity of conventional MRI in the evaluation of the heterogeneous pathological substrates of the disease, its inability to provide accurate estimates of damage outside focal lesions, and the fact that it cannot provide information on CNS functional reorganization after tissue injury has occurred. Advanced MRI techniques have allowed to identify novel markers of the disease, more closely linked to its pathological features, which may in part overcome the limitations of conventional MRI.

1.5.1. T2-hyperintense lesions

The characterization of WM lesion features suggestive of MS on conventional MR scans is central in the diagnostic work-up of patients suspected of having MS.[63] Typical MS lesions are round to ovoid in shape and range from a few millimeters to more than one or two centimeters in diameter.[63]

MS lesions typically develop in both hemispheres, but their distribution is often mildly asymmetric in the early stages. While lesions can occur in any CNS regions, relative to other disorders that cause WM lesions, MS lesions tend to affect specific WM regions, such as the periventricular and juxtacortical WM, the corpus callosum, infratentorial areas (especially the pons and the cerebellum) and the spinal cord (preferentially the cervical segment) (Figure 5).[63]

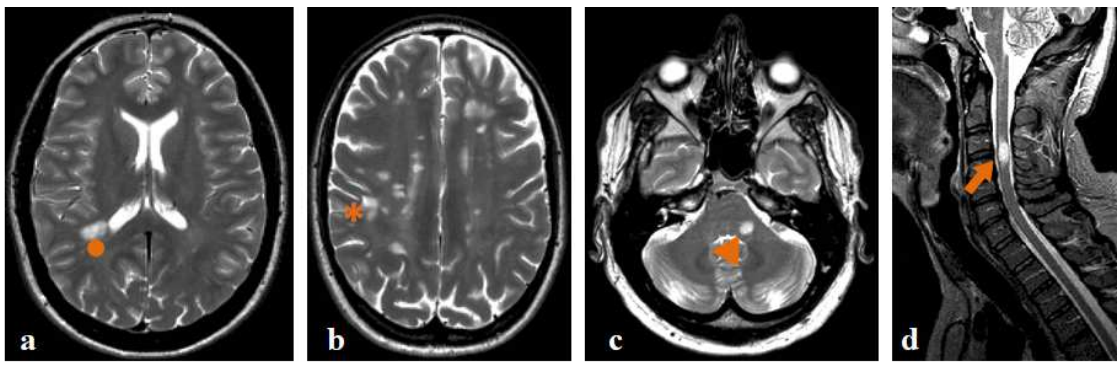

Figure 5. Typical brain and spinal cord MS lesions. (a) Periventricular (•), (b) juxtacortical (*), (c) infratentorial (arrowhead), and (d) spinal cord (arrow).

Lesion burden on T2w MRI scans of MS patients increases by about 5-10% per year. Several cross-sectional studies showed that T2-hyperintense LV is higher in SPMS in comparison to RRMS and PPMS.[93] However, the magnitude of the correlation between T2-hyperintense lesion burden and disability in cross-sectional studies remains disappointing. The presence of this so-called 'clinico-radiological paradox' might be due to the poor pathological specificity of T2-hyperintense lesions which do not distinguish oedema and inflammation from irreversible demyelination and axonal loss. This may also simply be a reflection of the fact that many T2-hyperintense lesions are clinically silent.[94] Of note, a plateauing relationship between T2-hyperintense LV and disability has been suggested for Expanded Disability Status Scale (EDSS) scores higher than 4.5.[95]

1.5.2. Gd-enhancing lesions

Serial MRI studies have shown that enhancement occurs in virtually all new lesions in patients with RRMS or SPMS and can sometimes be detected even before the onset of clinical symptoms (Figure 6).[96]

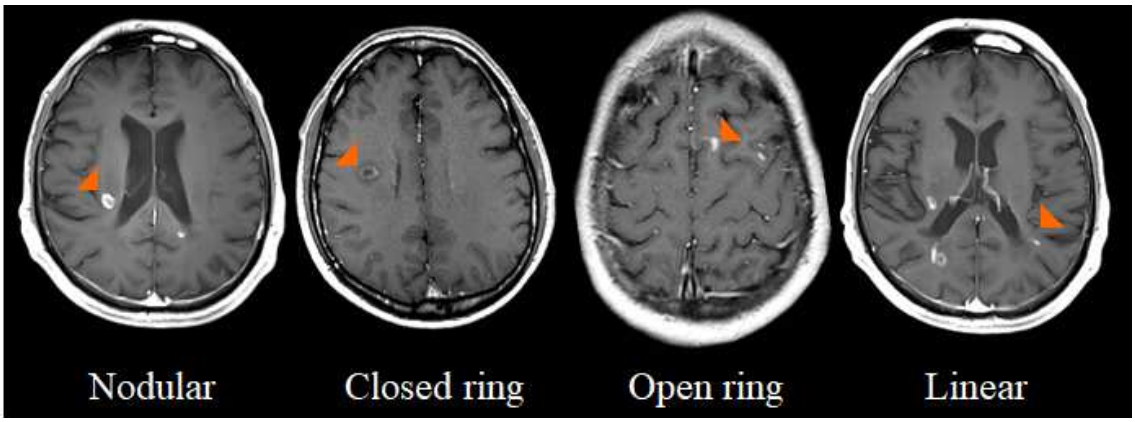

Figure 6. Typical patterns of Gd-enhancing lesions in MS.

The frequency of MRI activity varies according to the clinical phenotype of the disease, being higher in RRMS[97] and SPMS[98] than in PPMS.[98] Severely-disabled SPMS patients exhibit a substantially lower incidence of Gd-enhancing lesions when compared to those with RRMS,[99] even if the trend of enhancement might vary across different cohorts of patients with the same clinical phenotype of the disease.

The presence of Gd-enhancing lesions at disease onset, a marker of acute perivascular inflammation, also contributes to predict the development of physical disability at short and mid-term[86, 100, 101] in line with a higher number of relapses in the first years after disease onset.

Recently, using dynamic contrast-enhanced (DCE) MRI and ultra-high field magnets, different patterns of centrifugal and centripetal Gd-enhancement have been described,[102-104] suggesting a possible replacement of the previously accepted definition of nodular and ring-like lesions based on single post-Gd T1w scans in favour of a paradigm based on spatio-temporal enhancement dynamics. One of these studies[102] showed that centrifugal DCE lesions appear isointense or hypointense on phase images, whereas centripetal DCE lesions have thin, hypointense phase rims that clearly colocalize with the initial site of contrast enhancement. This hypointense rim was found to disappear in most lesions once enhancement resolved. On the contrary, chronic lesions showed stable hypointense phase rims which were typically thicker and darker than those seen in acute lesions. These findings suggest different underlying pathological processes in the two types of lesions.

1.5.3. T1-hypointense lesions

A subset of T2-hyperintense lesions (around 30-40%) appears persistently dark on post-contrast T1w images on serial scans and represent regions where irreversible axonal loss, demyelination and gliosis have occurred.[105-107] T1-hypointense lesions are only a few in the early stage of MS and increase over the course of the disease. Studies assessing the correlations between T1-hypointense lesion burden and disability provided conflicting results, since some of them found such a correlation to be stronger than for T2-hyperintense lesions, while others did not.[108]

1.5.4. Smoldering/slowly evolving lesions

Pathological studies show that up to 57% of chronic MS lesions are active or mixed (active and inactive).[24, 29, 109] These lesions may be characterized by a slow rate of increase in size and ongoing tissue loss, are more common in cases with long disease duration and PMS phenotypes and are termed smoldering or slowly evolving/expanding lesions. Pathologically, they are typified by a ‘rim’ of iron-laden microglia and/or

macrophages with altered morphology, activated microglia and macrophages at the edge, few T cells, and slow rate of ongoing demyelination and axonal loss.[24, 29, 31, 109]

Recently, these slowly evolving lesions have been investigated *in vivo* with MRI. Susceptibility-based MRI identifies a hypointense rim in some WM MS lesions that may reflect activity detected with pathology in the periphery of lesions. This rim can persist over years,[31, 34, 110-113] although it can also gradually disappear, returning similar to NAWM after some years.[114]

This hypointense rim is characteristic of lesions showing significant enlargement over time,[31] although expansion at the edge can be concurrent with volume loss within the lesion[115] or no volume change.[110]

Although T2* and phase images at ultra-high and high-field hold promise for identifying smoldering/slowly evolving lesions, at present there is no consensus about the best technique for use *in vivo*. A method based on the automatic detection of these lesions on conventional brain T2- and T1w images has recently been proposed.[116]

Interestingly, while slowly evolving lesions are common in MS, they are not found in NMOSD,[117, 118] or in cerebrovascular diseases.[119]

1.5.5. Brain and spinal cord atrophy

Neurodegeneration and irreversible tissue loss are among the pathologic hallmarks of MS and are clinically relevant, since they represent the main substrates determining the progression of locomotor disability and cognitive impairment.[108, 120]

With the acquisition of appropriate MRI sequences (typically high-resolution 3D T1w) and the application of optimized pipelines using segmentation-based and/or registration-based analyses, it is possible to quantify brain atrophy (an *in-vivo* measure of irreversible tissue loss) and its changes over time.[120]

In MS, a relevant atrophy occurs from the early stages of the disease at a rate of about 0.5%-1% per year compared to 0.1%-0.3% for healthy controls (HC).[120] While in the WM it is likely to reflect the loss of myelin, oligodendrocytes and axons, in the GM it is mainly due to neuro-axonal damage and loss.

Several findings have consistently demonstrated that brain atrophy measures are more pathologically specific than T2-hyperintense LV measurements and result in better correlations between clinical and MRI measures in MS patients, in terms of clinical

disability, cognitive impairment and other MS-related clinical manifestations, such as fatigue and depression.[108, 120]

Despite these promising findings, brain atrophy has several important limitations that prevent this measure to be applied in the clinical setting and for single-subject monitoring.[120] First, measurements of brain atrophy do not distinguish the different pathological substrates (e.g., demyelination, neuro-axonal loss, etc.). Second, reactive gliosis has the potential to mask considerable tissue loss. Third, brain atrophy fluctuates considerably due to several mechanisms, including physiologic factors (e.g., dehydration), development, resolution of inflammation and treatment effects (e.g., pseudo-atrophy). Fourth, atrophy is an end-stage phenomenon. Although detection of atrophy may be considered as a robust endpoint, the ability to monitor MS at a stage prior to irreversible tissue loss has occurred would be desirable.

1.5.6. Microstructural tissue abnormalities

Diffusion tensor (DT) and magnetization transfer (MT) MRI can quantify the extent and improve the characterization of the nature of microstructural abnormalities occurring within and outside focal MS lesions, since they are sensitive to the different pathophysiological substrates of the disease (demyelination, inflammation, and axonal loss).[121]

Diffusion-weighted (DW) MRI is a non-invasive imaging technique that exploits the diffusion of water molecules within biological tissues. The diffusion coefficient measures the ease of this translational motion of water. In biological tissues like the brain, this coefficient is lower than that in free water because the various structures of the tissues (membranes, cell bodies, glia, inclusions and macromolecules, etc.) influence the free movement of water molecules. For this reason, when diffusion is evaluated in such biological systems, the measured diffusion coefficient is referred to as the ‘apparent diffusion coefficient’ (ADC). Pathological processes that alter tissue integrity typically reduce the impediments to free water motion and, as a result, these processes tend to increase the measured ADC values. With an appropriate post-processing, the diffusion properties of the tissue, can be better characterized in terms of a tensor, which has a principal axis and two smaller axes which are perpendicular to each other and describe its width and depth.[121] The diffusivity along the principal axis is called parallel or axial

diffusivity (AD), while the diffusivities in the two minor axes are often averaged to produce a measure of radial diffusivity (RD). It is also possible to calculate the magnitude of diffusion, reflected by the mean diffusivity (MD), and the degree of anisotropy, which is a measure of tissue organization that can be expressed by several indexes, including a dimensionless one named fractional anisotropy (FA). The pathological elements of MS have the potential to alter the permeability or geometry of structural barriers to water diffusion in the CNS. Axonal damage has been suggested to alter predominantly FA and AD, while myelin breakdown has been associated with an increased RD even though pathologic studies have correlated myelin content also with FA and MD values.[122] Since different pathological substrates can influence such DT-derived indexes,[122] the results obtained from DT MRI should be interpreted with caution.[121]

Typically, increased MD and decreased FA have been described in lesions, NAWM and GM of MS patients, with more severe abnormalities in focal WM lesions, especially those hypointense on T1w images.[121] In these compartments, DT MRI abnormalities can be detected from the earliest stages of the disease, already in CIS patients, and they become more pronounced in PMS phenotypes, with increasing disease duration and neurologic impairment.[121]

MT MRI is based on the interactions between protons in free fluid and protons bound to macromolecules. When an off-resonance radio-frequency pulse is applied, the magnetization of bound protons becomes saturated. Magnetization is then transferred from these protons to more mobile protons, which reduces the signal intensity measured from the tissue. The MT ratio (MTR) reflects the efficiency of this exchange, since it quantifies the amount of MT exchange taking place between the free ('liquid') pool, in which protons are highly mobile, and a restricted ('semisolid') pool consisting of protons bound to macromolecules such as proteins or lipids, which are therefore relatively immobile. It is obtained by calculating the difference in signal intensity between the images acquired before (M_0 or not saturated) and after (M_S or saturated) the application of the radio-frequency pulse and then dividing this difference by the signal intensity before the pulse, according to the following formula: $(M_0 - M_S)/M_0 \times 100$. Therefore, a low MTR indicates that the signal reduction (due to the transfer of magnetization) is smaller than normal because of a reduced capacity of macromolecules in tissue to exchange magnetization with surrounding water molecules. As a consequence, this index

provides an estimate of the extent of MS tissue disruption. The most compelling evidence that the severity of MTR reduction reflects the severity of tissue injury comes from *post mortem* studies, which showed that MTR is strongly correlated with myelin alterations [123] but it may also be influenced by water content, inflammation and axonal density,[124] Typically, reduced MTR values have been found in NAWM and GM of MS patients, while more severe abnormalities have been reported in acute and chronic MS lesions, with the most prominent changes found in T1-hypointense lesions.[121] Lesional MTR is lower in the presence of demyelination, inflammation and axonal loss, while a significantly higher MTR is observed in remyelinated lesions.[121] MTR abnormalities have been consistently found more severe in the more disabling stages of the disease and correlate with the severity of clinical disability and cognitive impairment.[121]

1.5.7. MRI in MS diagnostic criteria

In 2001, MRI was formally included in the diagnostic algorithm for CIS patients with a suspicious of MS in the McDonald criteria.[74]

Since their introduction up to the recent 2017 revision,[4] the McDonald diagnostic criteria for MS have been based on the number, size and topography of brain and spinal cord lesions believed to be typical of MS[63] and assessed on conventional T2w and post-contrast T1w MRI sequences using standardized protocols.[64, 65]

The original criteria have been revised several times in the course of the past decade in an attempt to simplify them, to clarify specific aspects (e.g., the timing of follow-up [FU] evaluation, inclusion of spinal cord findings) and to simplify their use in the clinical setting.[4, 75, 76]

Based on new data about the application of MRI for the diagnosis of MS, in 2016 members of the European Magnetic Resonance Imaging in MS (MAGNIMS) group proposed evidence-based modifications to the MRI diagnostic criteria.[125, 126] These included removal of the distinction between symptomatic and asymptomatic MRI lesions for the definition of DIS and DIT; the need for three or more lesions to identify involvement of the periventricular region; the admission of an additional region (i.e., the optic nerve) for the definition of DIS; and the combined inclusion of both cortical and juxtacortical lesions in order to expand the concept of juxtacortical lesions for DIS.

These proposals helped to guide the latest revision of the MS diagnostic criteria (the 2017 revision of the McDonald criteria), where modifications included the removal of the distinction between symptomatic and asymptomatic lesions both for the assessment of DIS and DIT, the combination of cortical and juxtacortical lesions and the presence of CSF-specific OCBs as an additional DIT criterion (Table 1 and Figure 7).[4]

Table 1. The 2017 revised criteria for diagnosis of MS, adapted from Thompson et al.[4]

Clinical presentation	Additional data needed for MS diagnosis
≥ 2 clinical relapses and objective clinical evidence of ≥ 2 lesions; **OR** ≥ 2 clinical relapses and objective clinical evidence of 1 lesion and clear-cut historical evidence of a prior relapse involving a lesion in a distinct anatomic location	None
≥ 2 clinical relapses and objective clinical evidence of 1 lesion	**DIS**, demonstrated by: A second clinical relapse implicating a different CNS site **OR** demonstration of **DIS** by MRI (see Figure 7)
1 clinical relapse and objective clinical evidence of 2 or more lesions	**DIT**, demonstrated by: A second clinical relapse **OR** demonstration of DIT by MRI (see Figure 7) **OR** demonstration of CSF-specific OCBs
1 clinical relapse and objective clinical evidence of 1 lesion	**DIS** and **DIT**, demonstrated by: For **DIS**: A second clinical relapse implicating a different CNS site **OR** demonstration of **DIS** by MRI (see Figure 7)

	For **DIT**: A second clinical relapse **OR** demonstration of **DIT** by MRI (see Figure 7) **OR** demonstration of CSF-specific OCBs
Disease course characterized by progression from onset (PPMS)	One year of disability progression (retrospectively or prospectively determined) independent of clinical relapse Plus 2 out of 3 of the following criteria: • ≥1 T2-hyperintense lesions in ≥1 areas in the brain characteristic of MS (periventricular, cortical/juxtacortical or infratentorial) • ≥2 T2-hyperintense lesions in the spinal cord, with no distinction between symptomatic or asymptomatic lesions • Presence of CSF-specific OCBs

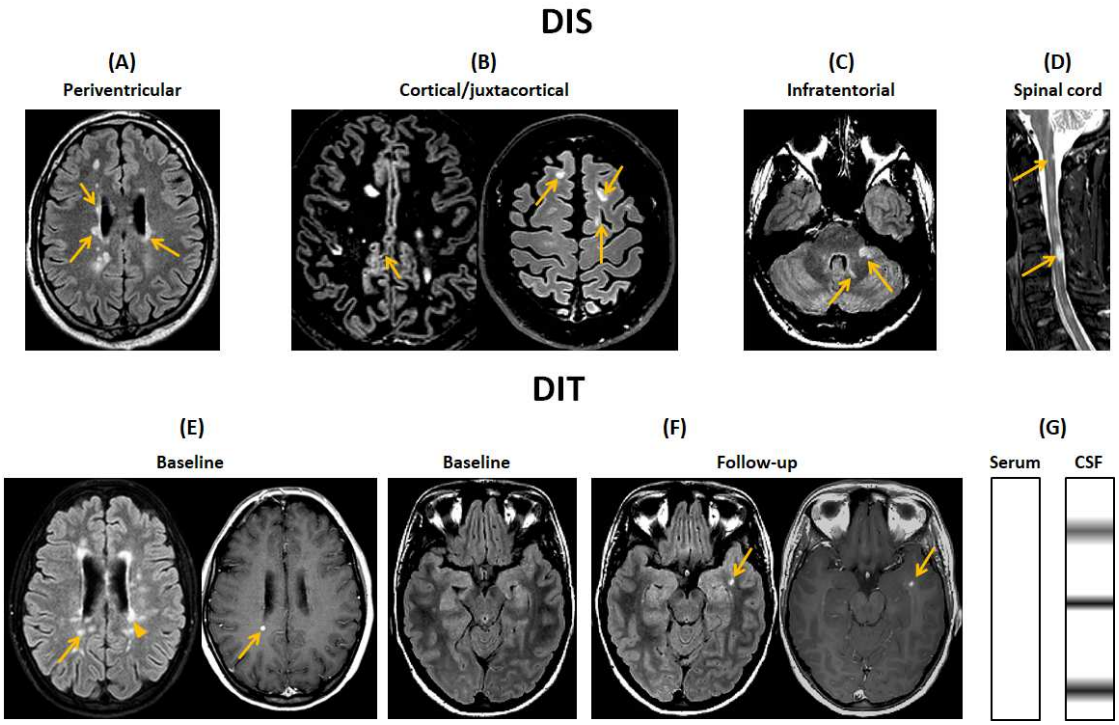

Figure 7. 2017 McDonald Criteria for demonstration of DIS and DIT in patients with a CIS suggestive of MS. Typical MRI examples (orange arrows) of (A) periventricular, (B) cortical/juxtacortical, (C) infratentorial and (D) spinal cord MS lesions. DIS can be demonstrated by ≥1 T2-hyperintense lesions in ≥2 of 4 typical areas of the central nervous system. DIT can be demonstrated by (E) a simultaneous presence of Gd-enhancing (orange arrows) and non-enhancing (orange arrowhead) lesions at any time; (F) a new T2-hyperintense and/or Gd-enhancing lesion on FU MRI (orange arrow), with reference to a baseline scan, irrespective of the timing of the baseline MRI; or (G) the presence of CSF-specific OCBs. For the definition of both DIS and DIT, the distinction between symptomatic and asymptomatic lesions has been removed in the 2017 revision of the McDonald criteria.

It is likely that, in the near future, MRI features more distinctive for MS could be applied to improve the specificity of MRI diagnostic criteria and to minimize the risk of misdiagnosis. For instance, the use of T2*-w gradient echo or susceptibility-w images MRI scans has shown that many MS lesions form around small vessels. The proportion of lesions showing a central vein ('central vein sign')[127] was found to be higher in MS compared to other conditions,[128] including NMOSD,[117, 129] CNS inflammatory vasculopathies,[130] migraine,[131] Susac syndrome,[132] cerebrovascular disease [119, 133-135] and incidental cerebral WM lesions.[136] In line with this, guidelines for the identification of the central vein sign and possible criteria to be included in the diagnostic work-up have been proposed,[127] although their validation is still needed.[63]

1.6. T1-weighted/T2-weighted-ratio

1.6.1. Pathological substrates

Recently, an MRI method based on the ratio of T1- and T2-w (i.e., T1w/T2w-ratio) image signal intensities, has been proposed to quantify brain myelin content,[137] since some evidence suggested that T1- and T2w signals are, respectively, positively and negatively associated with myelin content[138, 139] and may be particularly specific to this pathological substrate.[137] In particular, the myelin-related magnetic resonance contrast largely reflects differences in lipids[140] and free and myelin-bound water[141] concentration, but is also influenced by iron, particularly in T2*-weighted images. Since myelin and iron are strongly colocalized within the cortex,[142] it is reasonable to conclude that MR-based

signals across the cortical GM largely reflect myelin content both directly and indirectly.[137] By applying T1w/T2w-ratio, a good overlap was observed between cortical maps and the histological cortical myeloarchitecture in healthy subjects,[137, 143] and this was further supported by the demonstration of a moderate correlations between T1w/T2w-ratio and MTR, a measure that is considered specific for myelin damage quantification in MS patients.[144, 145]

However, more recent studies demonstrated a low correlation between T1w/T2w-ratio and myelin water fraction maps in the subcortical regions and no correlation in WM.[146] This may be also explained by the influence of other factors than myelin on T2 signal intensities, such as iron accumulation and inflammation and, by extension, T1w/T2w-ratio.[146, 147] Furthermore, the specificity of T1w/T2w-ratio for myelin was not confirmed by other studies in MS,[148-150] nor in other neurodegenerative diseases such as Alzheimer and Parkinson diseases.[151, 152] These discrepancies suggest that T1w/T2w-ratio may be sensitive to different pathological processes. In particular, two combined pathology-MRI studies found that T1w/T2w-ratio was significantly associated with dendrite[148] and neurite densities,[153] thus supporting the relevance of such a measure to detect neurodegeneration. Several factors could contribute to these conflicting results, particularly methodological heterogeneities in the T1w/T2w-ratio quantification must be taken into account.

1.6.2. Bias field correction

The T1w/T2w-ratio was proposed as able to self-correct for spatial differences in the receiver B_1 field (B_1^-) since these are similar for the two sequences and cancel out with the ratio. In first instance the effect of inhomogeneity in the transmit B_1 field (B_1^+) was considered minimal, at least for some specific scanner architecture and at relative low field strength (Figure 8).

Although the method requires a T1w and aT2w sequence only, the recommendation is still to use images with the same geometry for single center studies and with standardized parameters for multicenter acquisitions.[154] Patient movements should be avoided to allow a correct compensation of inhomogeneities and high resolution is required for the reconstruction of cortical layer surfaces.

A uniform B_1^+ field does not exclusively depend on the transmit coil, but on the head and body shape and dimensions and by the obtainable compensation via radiofrequency shimming. These effects increase with field strength and affect different sequences differently.[155]

The application of bias field correction methods is a possibility, however this can result in errors and it is likely to not sufficiently make differences between myelin layers in the GM visible.[137] Correction methods based on the measurements of a range of flip angles over the field of view[156] are more effective, but require additional scans and postprocessing (Figure 8). Moreover, the different local spatial distortions that vary between sequences imply that, because the ratio be effective as a correction, the two sequences should be as close as possible for resolution, geometry, bandwidth, k-space readout.

1.6.3. Calibrations

The T1w/T2w-ratio method is a relative measure potentially characterized by intensity scale inconsistencies across datasets, which may be present even for MRI images collected with the same scanner on different days.

To address this issue, different calibration approaches have been introduced.[157, 158] Ganzetti et al.[157] suggested a calibration algorithm based on image intensities outside the brain (i.e., eyeballs and temporal muscles). By applying a linear scaling procedure, an intensity histogram standardization of the ratio image can be obtained. Conversely, Misaki et al.[158] proposed a calibration based on the median GM intensity in the T1w and T2w images, producing intensity values ranging from −1 to 1, thus enabling to enhance delineation of tissue classes.[158]

Although calibration might be effective in a single center setting, it is important that the segmentation of the reference tissue is reproducible in all subjects without artifacts that are not rare for moving eyes. In multicenter studies, a linear scale may not be able to compensate for differences in contrast, resolution, filtering and contamination from weights other than pure T1 or T2 that might result from differences in sequence parameters.[154]

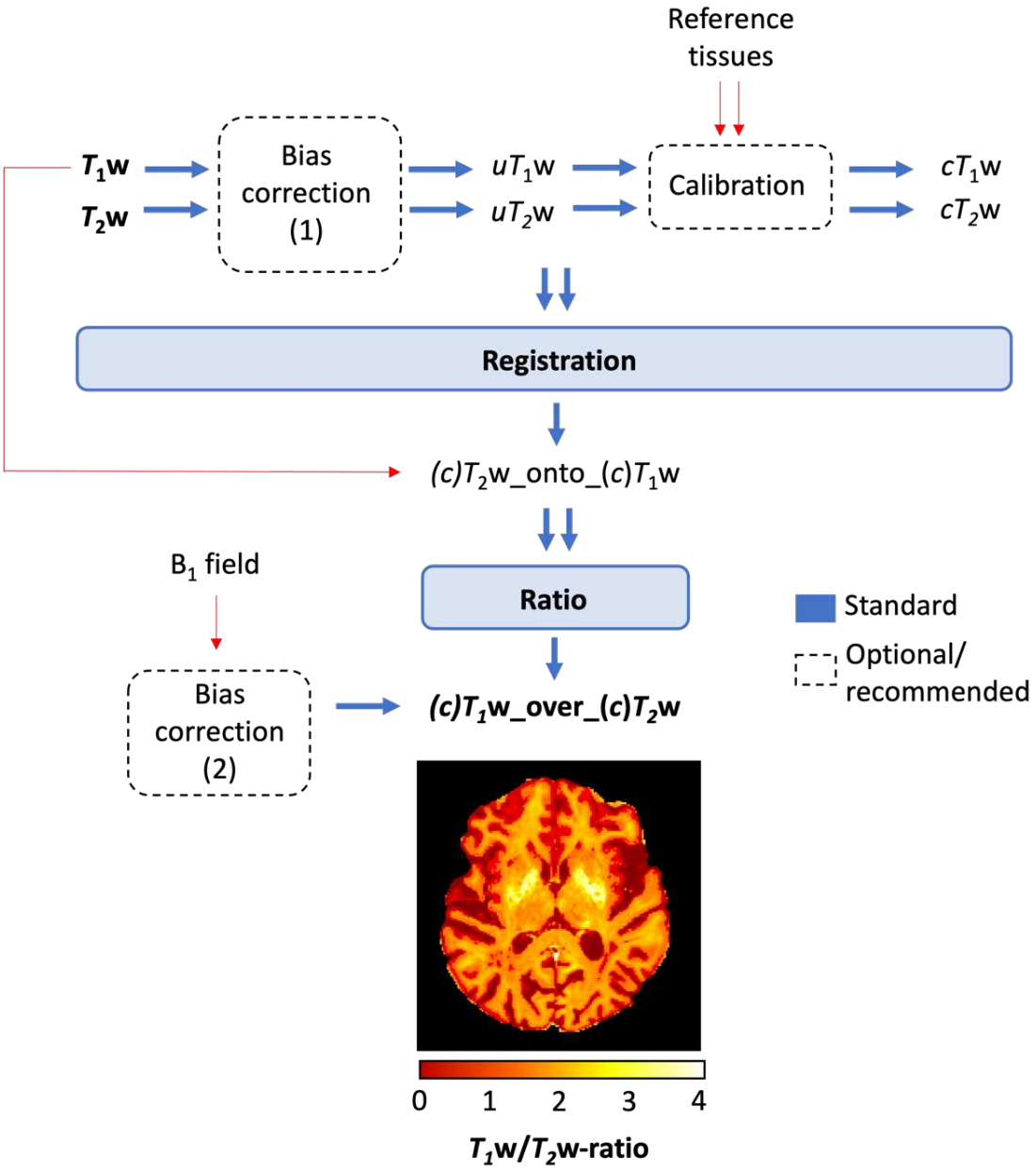

Figure 8. T1w/ T2w-ratio data processing, including standard (i.e., registration and ratio calculation) and optional/recommended (i.e., bias field correction, calibration) stages of the workflow.

Legend. *c*T1w = calibrated T1-weighted image; *c*T2w = calibrated T2-weighted image; *u*T1w = unbiased T1-weighted image; *u*T2w = unbiased T2-weighted image; w = weighted.

1.6.4. Clinical applications

At present, a few studies have investigated *in vivo* T1w/T2w-ratio in MS patients with conflicting results.[148, 159-166] T1w/T2w-ratio values were found significantly lower in the NAWM of early RRMS patients compared to HC.[160, 162, 166] However, this was not confirmed in other studies where no difference was detected in MS patients compared to HC [159, 161, 164]. Some studies found a significantly lower T1w/T2w-ratio in the cortex of RRMS and PMS patients,[148, 165] but not in the early phases of the disease.[164] So far, no study directly evaluated T1w/T2w-ratio in deep GM nuclei.

Furthermore, the clinical relevance of T1w/T2w-ratio still needs to be fully explored. A few studies in patients with mild disability and short disease duration showed mild correlations between EDSS and T1w/T2w-ratio in the NAWM and cortex.[148, 160] Several factors could contribute to these conflicting results. Methodological heterogeneities in the T1w/T2w-ratio quantification must be taken into account.[137, 157] Moreover, some studies evaluated small cohorts of MS patients, not spanning the whole spectrum of disease severity and with limited age-range.

2. AIMS OF THE STUDY

Based on the previous considerations, there is the need to investigate T1w/T2w-ratio in the different brain compartments in a wider cohort of MS patients with different ages and disease clinical phenotypes, and to evaluate its feasibility and clinical relevance in a multicenter setting.

The aims of this study were to characterize T1w/T2w-ratio in different brain tissues in a large multicenter dataset of HC and MS patients across the lifespan and spanning the main clinical phenotypes and to assess the relationship between T1w/T2w-ratio and clinical disability.

3. MATERIAL AND METHODS

3.1. Participants

Participants were retrospectively identified at 7 European centers (http://www.magnims.eu/): (1) the Amsterdam MS Center (the Netherlands); (2) the CEM-Cat, Hospital Vall d'Hebron, Barcelona (Spain); (3) Institute of Neurology, UCL, London (UK); (4) the Neuroimaging Research Unit, IRCCS San Raffaele Scientific Institute, Milan (Italy); (5) the MRI Center "SUN-FISM," University of Campania "Luigi Vanvitelli," Naples (Italy); (6) the Nuffield Department of Clinical Neurosciences, Oxford (UK); and (7) the Clinic of Neurology, Faculty of Medicine, University of Belgrade, Belgrade (Serbia).

To be included, MS patients had to have stable treatment during the last 6 months prior to imaging and received no corticosteroids during the last month. Patients with a CIS suggestive of MS had to have a first episode suggestive of CNS demyelination and a clinical assessment within 3 months from clinical symptoms onset. A diagnosis of neuromyelitis optica or of other conditions mimicking MS were carefully excluded from the study. HC were recruited among spouses of patients and by word of mouth. Exclusion criteria for both HC and MS were major comorbidities (i.e., cerebrovascular disease, psychiatric disorders); history of drug/alcohol abuse and contraindications to undergo MRI (i.e., claustrophobia, metal implants, pacemakers, pregnancy or breastfeeding).

3.1.1. Standard protocol approvals, registrations, and patient consents

Approval was received from the local ethical standards committees at each participating center; written informed consent was obtained from all study participants prior to enrollment. A MAGNIMS data-sharing agreement was signed among the participating centers.

3.2. Clinical assessment

Within 48 hours from MRI acquisition, MS patients underwent a complete neurologic evaluation, with definition of the clinical phenotype, rating of the EDSS score[167] and recording of disease-modifying treatments (DMTs). The clinical assessment was performed at each site by an experienced neurologist, unaware of the MRI results.

3.3. MRI acquisition

Using 3T scanners (Siemens [Erlangen, Germany] Magnetom Trio in Barcelona; Magnetom Prisma in Oxford; Philips [Best, the Netherlands] Achieva in Milan, and London; General Electric [Fairfield, CT] Signa HDtx in Amsterdam and Naples and a 1.5T scanner (Philips [Best, the Netherlands] Achieva in Belgrade (all without software/hardware upgrades during the study), the following brain sequences were acquired from all subjects during a single session: (1) brain 3-dimensional T1-weighted scan (repetition time [TR] range 6.9–7.0 milliseconds [ms] for GE and Philips and 2040–2300 ms for Siemens, echo-time [TE] range 2.8–4.7 ms, inversion time [TI] range 450–1000 ms, flip angle [FA] range 8°–12°, 128 to 204 sagittal slices with 1.0- to 1.2 millimeters (mm) slice thickness and ≈1 mm^2 in-plane resolution), (2) axial brain 2-dimensional dual-echo fast spin-echo (TR range 2500–4670 ms, TE range 16–27/80–120 ms, FA range 90°–150°, 44 to 47 axial slices with 3 mm slice thickness and ≈0.3- to 1.0-mm^2 in-plane resolution) or brain 3-dimensional T2w scan (TR range 2300–2500 ms, TE range 112-330 ms, FA variable, 192 axial slices with 0.8-1 mm slice thickness and ≈0.8-1.0-mm^2 in-plane resolution), (3) sagittal 3D fluid attenuation inversion recovery (FLAIR) (TR=4800 ms, TE=270 ms, inversion time [TI]=1650 ms, 192 slices with 1 mm slice thickness and 1.0 mm^2 in-plane resolution).

See Table 2 for additional details regarding scan geometry.

Table 2. Main MRI sequence parameters used at the participating sites.

Brain sequence	Parameters	Amsterdam (GE)	Barcelona (Siemens)	Belgrade (Philips)	London (Philips)	Milan I (Philips)	Milan II (Philips)	Naples (GE)	Oxford (Siemens)
3D T1-weighted	TR/TE [ms]	7.8/3	2300/2.98	7/3.2	6.9/3.14	7/3.2	7/3.2	6.9/2.8	2040/4.7
	TI [ms]	450	900	1000	"shortest"	1000	900	650	900
	FA [degree]	12	9	8	8	8	8	8	8
	FOV [mm]	240×240	256×256	256x256	256×256	256×256	256×240	260×260	192×174
	Pixel size [mm]	1×1×1	1×1×1.2	1×1×1	1×1×1	1×1×1	1×1×1	1.01×1.01×1.2	1×1×1
	# slices	176	128	180	180	204	192	166	192
	Thickness [mm]	1	1.2	1	1	1	1	1.1	1
	Orientation	Sag	Sag	Sag	Sag	Sag	Sag	Sag	Tra
3D T2-weighted or 2D T2-weighted DE-FSE	TR/TE [ms]	2300/112	2500/16-91	3130/20-100	3500/18-85	2500/330	2910/16-80	3080/24-120	4670/27-106
	FA [degree]	variable	123	90	90	8	90	90	150
	FOV [mm]	256×256	250×250	240×192	240×240	256×256	240×240	240×240	256×184
	Pixel size [mm]	0.8×0.8×0.8	0.78×0.78×3.0	0.94×0.94×0.94	1.0×1.0×3.0	1.21×1.21×1.21	0.93×0.93×3.0	0.47×0.47×3.0	0.34×0.34×3.0
	# slices	192	46	44	50	192	50	44	47
	Thickness [mm]	0.8	3	3	3	1	3	3	3
	Orientation	Sag	Tra	Tra	Tra	Sag	Tra	Tra	Tra
3D FLAIR	TR/TE [ms]	-	-	-	-	4800/270	-	-	-
	TI [ms]	-	-	-	-	1650	-	-	-
	FA [degree]	-	-	-	-	90	-	-	-
	FOV [mm]	-	-	-	-	256×256	-	-	-
	Pixel size [mm]	-	-	-	-	1×1×1	-	-	-
	# slices	-	-	-	-	192	-	-	-
	Thickness [mm]	-	-	-	-	1	-	-	-
	Orientation	-	-	-	-	Sag	-	-	-

Abbreviations: 3D=three-dimensional; 2D=two-dimensional; DE-FSE=dual-echo fast spin-echo; FA=flip angle; FLAIR=fluid attenuated inversion recovery; FOV=field of view; GE=General Electrics; ms=millisecond; PD=proton density; Sag=sagittal; TE=echo-time; TI=inversion time; TR=repetition time; Tra=transverse.

3.4. MRI analysis

3.4.1. Conventional MRI analysis

Brain T2-hyperintense LV was measured on the dual-echo or FLAIR scans, using, respectively, a local thresholding segmentation technique (n=562) (Jim 8, Xinapse Systems) or a fully automated deep-learning approach (n=142).[168] Normalized brain volume (NBV), WM volume (NWMV), GM volume (NGMV) and cortical GM volume were measured on the 3D T1w scans using the SIENAx2 software,[169] after T1-hypointense lesion filling.[170, 171] Deep GM nuclei (i.e., thalamus, caudate, putamen, pallidum) were segmented from the lesion-filled brain 3D T1w images using FSL FIRST.[172] Masks of the aforementioned brain regions were then derived. GM maps were thresholded at probability value of 0.5 to limit partial volume effects from WM and CSF. The results of segmentation were all visually checked. The caudate and putamen together comprised the striatum.

As performed in previous studies,[173, 174] volume of deep GM nuclei was calculated and normalized using FSL SIENAx scaling factor.

3.4.2. T1w/T2w-ratio image reconstruction

To obtain T1w/T2w-ratio maps, 3D T1w and T2w images were preprocessed and combined using an in-house dedicated pipeline adapted from Ganzetti et al.[157] This included intensity bias correction and calibration of each of the two input MRI sequences and the subsequent calculation of their ratio. In detail, first, 3D T1w and T2w images underwent intensity N4 bias field correction.[175] Then, 3D T1w and T2w images were further processed to normalize their signal intensity histograms using a linear scaling procedure described in Ganzetti et al. (implemented in Matlab® v2012).[157] Specifically, the intensity histograms were anchored using the lowest and the highest intensity peaks derived from the ocular and temporal muscle masks that were defined manually in MNI space to improve the overlap with anatomy. The normalized signal intensity maps were then extracted from both T1- and T2w images after non-linear registrations of the tissue masks into the subject space (http://stnava.github.io/ANTs/). The co-registrations of the masks in the subject's space were checked by visual inspection. The intensity bias-corrected and calibrated T2w image was then co-registered to the 3D T1w image space

through a rigid-body transformation using FLIRT tool (FSL Library). The ratio between these images was calculated in native space.

T1w/T2w-ratio values within the cortical and deep GM were derived by imposing the previously obtained tissue segmentation masks on the T1w/T2w-ratio image. T1w/T2w-ratio values of cortical GM above the 99th percentile were excluded from the analysis.

To extract T1w/T2w-ratio values from WM lesions, the transformation estimated by co-registering T1- and T2w images was applied to the WM lesion masks. T1w/T2w-ratio values within the NAWM were also derived after removing lesions from the WM mask.

3.5. Statistical analysis

Demographic and clinical variables were compared between groups using Chi-squared, Kruskal-Wallis and Mann-Whitney tests, or linear models, as appropriate. Age- and sex-adjusted linear mixed models for clustered data (participants within sites) were performed to assess differences in MRI features between HC and MS patients, as well as between clinical phenotypes, with the following a priori contrasts: RRMS *vs* CIS, SPMS *vs* RRMS, and SPMS *vs* PPMS. Brain T2-hyperintense LV was log-transformed.

To estimate T1w/T2w-ratio expected lifespan trajectories in different brain compartments, we fitted linear mixed models, accounting for clustering (participants within sites), to HC data. Sex, age and age squared were included as fixed effects according to Akaike information criterion. We dealt with heterogeneity in residual variances, due to different T2w sequences geometry, by allowing heteroscedastic errors. First-order derivative (estimated slope) of each model was evaluated across ages (steps of 5 years) to assess the rates of T1w/T2w-ratio changes.

Estimated parameters from the described models were then used to convert T1w/T2w-ratio values measured in MS patients to z-scores, which are relative to healthy sex- and age-corrected values from HC. In particular, they represent a standardized measure of deviation from the sex-, age- and site-specific expected values in the HC population. We assessed (testing the nullity, i.e., healthy population reference value, of the estimated means) and compared z-scores in MS patients as a whole and in clinical phenotypes, by linear models. Obtained results suggested stratifying MS patients according to the relapse-onset continuum (i.e., CIS, RRMS, SPMS) or progressive-onset (i,e., PPMS) course. Therefore, we studied by linear regression models z-scores trends along increasing disability levels. To this aim, we chose the following EDSS scores, considered relevant milestones of disease severity: (1) EDSS=3.0 (fully ambulatory, with mild disability in 3 or 4 functional systems [FS] or moderate disability in one FS); (2) EDSS=4.0 (ambulatory for at least 500 meters, despite severe disability in one FS, or other combinations of moderate disability in other FS); and (3) EDSS=6.0 (unilateral assistance to walk 100 meters). Lastly, we ran linear regression models to investigate the association of T1w/T2w-ratio in different brain compartments with disease duration and EDSS. Differences of associations between relapse-onset and progressive-onset MS

patients were tested by interaction terms. A random intercept for site was added to assess the association with brain T2-hyperintense LV and NBV.

All the analyses were repeated including the presence of DMT as a binary variable in our models. The significance of specific interaction terms was also tested.
Benjamini-Hochberg false discovery rate (FDR) correction was carried out to account for the overall number of tests performed, for each analysis separately.

SAS release 9.4 (SAS Institute, Cary, NC) was used for computations. P-values<0.05 were deemed statistically significant.

4. RESULTS

4.1. Demographic, clinical and conventional MRI findings

Table 3 summarizes the main demographic, clinical and conventional MRI findings from HC and MS patients included in the study.

Among the 275 HC and 444 MS patients initially evaluated for the study, 5 HC and 10 MS patients were excluded due to the incomplete MRI protocol (n=5) or inadequate MRI scan quality (poor positioning, movement artefacts, n=10). Ultimately, data from 270 HC and 434 MS patients were available for analysis, including 57 CIS, 196 RRMS, 106 SPMS and 75 PPMS.

Compared to HC, MS patients were significantly older ($p=0.009$), and as expected had significant higher brain T2-hyperintense LV, and lower NBV, NGMV, normalized cortical GMV, NWMV, as well as lower normalized thalamic, striatum and pallidum volumes (FDR $p<0.001$ for all).

Compared to CIS, RRMS patients had a higher EDSS score ($p=0.001$), longer disease duration ($p<0.001$), higher brain T2-hyperintense LV (FDR $p<0.001$), and lower NBV, NGMV, normalized cortical GM volume, normalized thalamic, pallidum and striatum volumes (FDR p ranging from <0.001 to 0.028).

Compared to RRMS, SPMS patients had a higher EDSS, longer disease duration, higher brain T2-hyperintense LV ($p<0.001$ for all), and lower NBV, NWMV, NGMV, normalized cortical GM volume, normalized thalamic, pallidum and striatum volumes (FDR p ranging from <0.001 to 0.011).

Compared to SPMS, PPMS patients had shorter disease duration ($p<0.001$). Compared to PPMS, SPMS patients had a higher brain T2-hyperintense LV (FDR $p=0.024$) and lower NBV, NGMV, NWMV, normalized thalamic, pallidum and striatum volumes (FDR p ranging from <0.001 to 0.042).

Table 3. Main demographic, clinical, and conventional MRI characteristics of HC and MS patients as a whole, and according to their disease clinical phenotype.

Variable		HC (n=270)	All MS (n=434)	P (FDR p)	CIS (n=57)	RRMS (n=196)	SPMS (n=106)	PPMS (n=75)	p[a]
Sex									
Male (%)		121 (45)	177 (41)	0.293	18 (32)	78 (40)	42 (40)	39 (52)	0.131
Female (%)		149 (55)	257 (59)		39 (68)	118 (60)	64 (60)	36 (48)	
Mean age (SD) [years]		41.9 (15.4)	44.8 (12.2)	**0.009**	32.4[b] (8.8)	42.7[c] (11.3)	53.1[d] (8.6)	48.1[b,e] (11.7)	**<0.001**
Median disease duration (IQR) [years]			12.0 (2.6;20.2)	-	0.4 (0.3;1.0)	12.7[c] (4.5;19.3)	20.8[d] (15.0;27.0)	6.0[e] (2.0;16.0)	**<0.001**
Median EDSS (IQR)			3.5 (1.5;5.5)	-	1.5 (1.0;2.0)	2.0[c] (1.5;3.0)	6.0[d] (5.0;6.5)	5.5 (4.0;6.5)	**<0.001**
Patients receiving DMTs (%)			221 (51)	-	5 (9)	172[c] (88)	29[d] (27)	15 (20)	**<0.001**
Median brain T2-hyperintense LV (IQR) [mL]		0.1 (0.0;0.2)	5.0 (2.2;12.5)	-	3.1 (2.5;3.6)	3.7[c] (3.4;4.0)	4.1[d] (3.7;4.4)	3.7[e] (3.4;4.1)	**<0.001**
Estimated mean	**NBV (SE) [mL]**	1569 (12)	1523 (12)	**<0.001 (<0.001)**	1551[b] (12)	1528[c] (11)	1493 (12)	1522[e] (13)	**<0.001**
	NWMV (SE) [mL]	707 (18)	690 (18)	**<0.001 (<0.001)**	701 (18)	693 (18)	677[d] (18)	691[e] (18)	**<0.001**
	NGMV (SE) [mL]	862 (16)	833 (16)	**<0.001 (<0.001)**	848[b] (16)	836[c] (15)	818[d] (16)	832[e] (16)	**<0.001**
	Normalized cortical volume (SE) [mL]	650 (11)	625 (11)	**<0.001 (<0.001)**	638[b] (11)	626[c] (10)	612[d] (11)	623 (11)	**<0.001**
	Normalized thalamic volume (SE) [mL]	22.1 (0.4)	20.3 (0.4)	**<0.001 (<0.001)**	21.7 (0.4)	20.4[c] (0.4)	19.0[d] (0.4)	20.3[e] (0.5)	**<0.001**
	Normalized striatum volume (SE) [mL]	23.6 (0.3)	21.9 (0.3)	**<0.001 (<0.001)**	23.5 (0.4)	21.8[c] (0.3)	21.0[d] (0.4)	21.8[e] (0.4)	**<0.001**
	Normalized pallidum volume (SE) [mL]	4.9 (0.1)	4.7 (0.1)	**<0.001 (<0.001)**	5.0 (0.1)	4.7[c] (0.1)	4.4[d] (0.1)	4.7 (0.1)	**<0.001**

Comparisons performed by Chi-squared (sex), Kruskal-Wallis and Mann-Whitney (disease duration and EDSS) tests, and linear models (age). FDR correction (Benjamini-Hochberg procedure) was applied to account for the overall number of tests. Age- and sex-adjusted linear mixed models, for clustered data (participants within sites), were performed for MRI features. Bold values denote statistical significance ($p<0.05$).

p[a]Heterogeneity among MS phenotypes.
[b]Significant post hoc comparisons vs HC.
[c]Significant post hoc comparisons vs CIS.
[d]Significant post hoc comparisons vs RRMS.
[e]Significant post hoc comparisons vs SPMS.

Abbreviations: CIS=clinically isolated syndrome; DMT=disease-modifying therapy; EDSS = Expanded Disability Status Scale; HC=healthy controls; LV=lesion volume; MRI=magnetic resonance imaging; NBV=normalized brain volume; NGMV=normalized gray matter volume; NWMV=normalized white matter volume; PPMS=primary progressive multiple sclerosis; RRMS = relapsing-remitting multiple sclerosis; SPMS=secondary progressive multiple sclerosis.

4.2. T1w/T2w-ratio trajectories in healthy controls

Estimated sex- and site-adjusted T1w/T2w-ratio trajectories and their slope in the different brain compartments in HC are shown in Figure 9 and Table 4. The T1w/T2w-ratio significantly increased until the age of 45 years in the thalamus, until 50 years in the WM and pallidum and until 60 years in the cortex and striatum (FDR p ranging from <0.001 to 0.022). Interestingly, a steep slope was detected in the first decades especially in the pallidum and striatum.

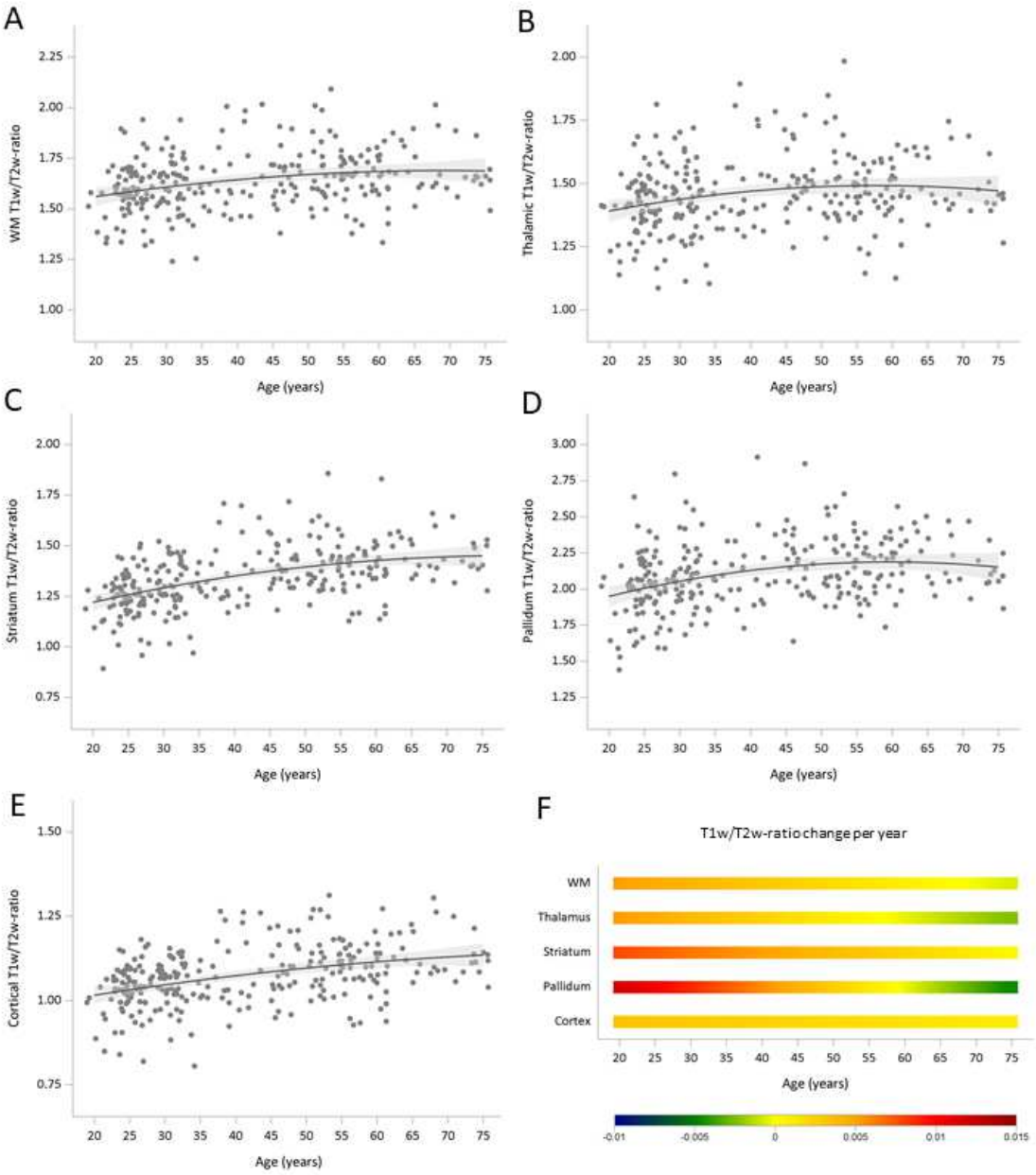

Figure 9. Estimated sex- and site-adjusted T1w/T2w-ratio lifespan trajectories in different brain compartments of HC. The figure shows T1w/T2w-ratio mean estimated sex- and site-adjusted values (solid lines with 95% shaded confidence intervals) in (A) WM, (B) thalamus, (C) striatum, (D) pallidum and (E) cortex, across ages in HC (linear mixed models). (F) Rates of T1w/T2w-ratio change (trajectories estimated slopes) across ages in the different brain compartments studied in HC.

Abbreviations: HC=healthy controls; T1w/T2w-ratio=T1weighted/T2weighted-ratio; WM=white matter.

Table 4. Mean estimated T1w/T2w-ratio values across ages (steps of 5 years) from sex- and site-adjusted lifespan trajectories in different brain compartments of HC. The first-order derivative (estimated slope) of the model is also shown, to assess T1w/T2w-ratio change rate.

	Age	Estimated mean (SE)	95% CI	Estimated slope (SE) [x10^{-3}]	p (FDR p)*
WM	20	1.560 (0.023)	1.514;1.606	5.247 (2.055)	**0.011 (0.019)**
	25	1.585 (0.016)	1.553;1.616	4.712 (1.704)	**0.006 (0.011)**
	30	1.607 (0.012)	1.583;1.631	4.177 (1.363)	**0.002 (0.006)**
	35	1.626 (0.012)	1.604;1.649	3.642 (1.046)	**0.001 (0.002)**
	40	1.643 (0.013)	1.618;1.668	3.107 (0.781)	**<0.001 (<0.001)**
	45	1.657 (0.014)	1.630;1.685	2.572 (0.637)	**<0.001 (<0.001)**
	50	1.669 (0.015)	1.640;1.698	2.037 (0.692)	**0.004 (0.007)**
	55	1.678 (0.015)	1.648;1.708	1.502 (0.912)	0.102 (0.149)
	60	1.684 (0.016)	1.652;1.716	0.966 (1.210)	0.426 (0.511)
	65	1.687 (0.019)	1.649;1.726	0.431 (1.542)	0.780 (0.816)
	70	1.688 (0.025)	1.639;1.737	-0.100 (1.889)	0.956 (0.958)
	75	1.686 (0.033)	1.621;1.751	-0.640 (2.245)	0.776 (0.816)
Thalamus	20	1.390 (0.022)	1.347;1.434	5.331 (1.954)	**0.007 (0.012)**
	25	1.415 (0.015)	1.385;1.446	4.626 (1.621)	**0.005 (0.009)**
	30	1.437 (0.012)	1.414;1.459	3.922 (1.298)	**0.003 (0.006)**
	35	1.455 (0.011)	1.433;1.476	3.217 (0.997)	**0.001 (0.003)**
	40	1.469 (0.012)	1.445;1.493	2.512 (0.744)	**0.001 (0.002)**
	45	1.480 (0.013)	1.454;1.506	1.808 (0.604)	**0.003 (0.006)**
	50	1.487 (0.014)	1.459;1.515	1.103 (0.653)	0.093 (0.139)
	55	1.491 (0.014)	1.462;1.519	0.399 (0.859)	0.643 (0.715)
	60	1.491 (0.016)	1.460;1.522	-0.310 (1.140)	0.789 (0.816)
	65	1.488 (0.018)	1.452;1.524	-1.010 (1.454)	0.488 (0.559)
	70	1.481 (0.023)	1.435;1.527	-1.720 (1.783)	0.337 (0.422)
	75	1.471 (0.031)	1.409;1.532	-2.420 (2.120)	0.255 (0.340)
Striatum	20	1.219 (0.02)	1.180;1.259	7.829 (1.738)	**<0.001 (<0.001)**
	25	1.257 (0.014)	1.230;1.284	7.163 (1.442)	**<0.001 (<0.001)**
	30	1.291 (0.01)	1.271;1.311	6.498 (1.155)	**<0.001 (<0.001)**
	35	1.322 (0.01)	1.303;1.341	5.832 (0.888)	**<0.001 (<0.001)**

	40	1.349 (0.011)	1.328;1.371	5.167 (0.663)	**<0.001 (<0.001)**
	45	1.374 (0.012)	1.350;1.397	4.502 (0.537)	**<0.001 (<0.001)**
	50	1.394 (0.012)	1.370;1.419	3.836 (0.579)	**<0.001 (<0.001)**
	55	1.412 (0.013)	1.386;1.437	3.171 (0.762)	**<0.001 (<0.001)**
	60	1.426 (0.014)	1.399;1.453	2.506 (1.011)	**0.014 (0.022)**
	65	1.437 (0.016)	1.405;1.469	1.840 (1.290)	0.156 (0.222)
	70	1.445 (0.021)	1.403;1.486	1.175 (1.582)	0.459 (0.540)
	75	1.449 (0.028)	1.394;1.503	0.509 (1.881)	0.787 (0.816)
Pallidum	20	1.948 (0.036)	1.878;2.019	12.020 (3.147)	**<0.001 (0.001)**
	25	2.004 (0.025)	1.956;2.053	10.510 (2.610)	**<0.001 (<0.001)**
	30	2.053 (0.019)	2.017;2.090	8.990 (2.089)	**<0.001 (<0.001)**
	35	2.094 (0.018)	2.059;2.129	7.476 (1.604)	**<0.001 (<0.001)**
	40	2.128 (0.019)	2.090;2.166	5.961 (1.198)	**<0.001 (<0.001)**
	45	2.154 (0.021)	2.112;2.196	4.446 (0.974)	**<0.001 (<0.001)**
	50	2.172 (0.022)	2.128;2.217	2.931 (1.056)	**0.006 (0.011)**
	55	2.183 (0.023)	2.137;2.229	1.417 (1.391)	0.310 (0.396)
	60	2.187 (0.025)	2.137;2.236	-0.100 (1.845)	0.958 (0.958)
	65	2.182 (0.030)	2.124;2.241	-1.610 (2.351)	0.494 (0.559)
	70	2.170 (0.038)	2.096;2.245	-3.130 (2.882)	0.279 (0.364)
	75	2.151 (0.050)	2.052;2.250	-4.640 (3.426)	0.177 (0.247)
Cortex	20	1.016 (0.013)	0.990;1.041	3.314 (1.122)	**0.004 (0.007)**
	25	1.032 (0.009)	1.014;1.049	3.105 (0.931)	**0.001 (0.002)**
	30	1.047 (0.007)	1.034;1.060	2.896 (0.745)	**<0.001 (<0.001)**
	35	1.061 (0.006)	1.048;1.073	2.688 (0.572)	**<0.001 (<0.001)**
	40	1.073 (0.007)	1.060;1.087	2.479 (0.427)	**<0.001 (<0.001)**
	45	1.085 (0.008)	1.070;1.100	2.271 (0.347)	**<0.001 (<0.001)**
	50	1.096 (0.008)	1.080;1.112	2.062 (0.376)	**<0.001 (<0.001)**
	55	1.106 (0.008)	1.090;1.122	1.853 (0.494)	**<0.001 (0.001)**
	60	1.115 (0.009)	1.097;1.132	1.645 (0.656)	**0.013 (0.021)**
	65	1.122 (0.011)	1.102;1.143	1.436 (0.837)	0.088 (0.135)
	70	1.129 (0.013)	1.102;1.156	1.227 (1.026)	0.233 (0.318)
	75	1.135 (0.018)	1.099;1.170	1.019 (1.219)	0.405 (0.495)

Linear mixed effect model accounting for clustering (participants within sites), including sex, age and age square as fixed effects, according to Akaike information criterion.

*p values of the test for the nullity of the slope. FDR correction (Benjamini-Hochberg procedure) was applied to account for the overall number of tests. Bold values denote statistical significance ($p<0.05$).
Abbreviations: CI=confidence interval; FDR=false discovery rate; HC=healthy controls; SE=standard error; WM=white matter.

4.3. T1w/T2w-ratio in multiple sclerosis clinical phenotypes

Between-group comparisons in the T1w/T2w-ratio z-scores of the different brain compartments are summarized in Table 5 and Figure 10.

Compared to HC WM, T1w/T2w-ratio was significantly lower in T2-hyperintense WM lesions of MS patients, including all the main clinical phenotypes (FDR $p<0.001$ for all). Similarly, T1w/T2w-ratio of NAWM and cortex were significantly lower in MS patients compared to HC (FDR $p=0.001$ for both), although this was significant only in RRMS and SPMS patients when the clinical phenotypes were evaluated separately (FDR p ranging from 0.001 to 0.026).

Conversely, T1w/T2w-ratio of the pallidum and striatum were significantly higher in MS patients compared to HC (FDR $p\leq0.001$). In the analysis according to disease clinical phenotype, such a difference was detected only in RRMS, SPMS and PPMS patients (FDR p ranging from 0.001 to 0.042).

Thalamic T1w/T2w-ratio did not differ between MS patients and HC, also according to disease clinical phenotypes (FDR $p\geq0.355$).

T2-hyperintense WM lesion T1w/T2w-ratio was significantly lower in SPMS *vs* RRMS (FDR $p=0.004$), whereas T1w/T2w-ratio of the striatum and pallidum were significantly higher in SPMS *vs* RRMS (FDR $p=0.045$ and 0.002, respectively).

T1w/T2w-ratio did not differ between RRMS *vs* CIS or between PPMS *vs* SPMS (FDR $p\geq0.392$) in any gray or WM region.

Results did not change when adjusting for treatment. No influence of DMT on T1w/T2w-ratio within-group estimates ($p\geq0.071$) and between-phenotypes comparisons ($p\geq0.222$) was detected.

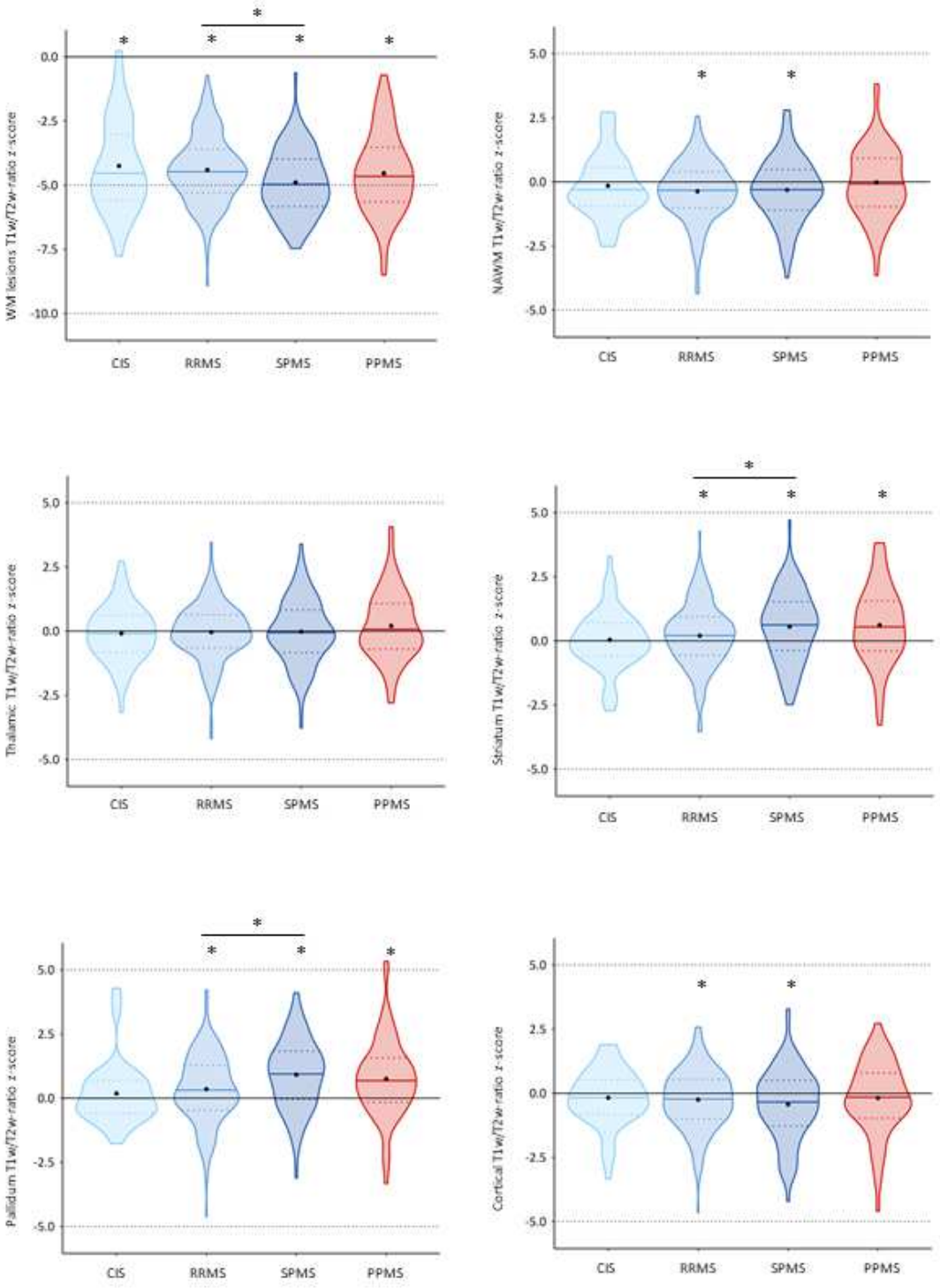

Figure 10. T1w/T2w-ratio z-scores distribution in MS patients according to their clinical phenotype in different brain compartments. Violin plots show the distribution of T1w/T2w-ratio z-scores in (A) WM lesions, (B) NAWM, (C) thalamus, (D) striatum, (E) pallidum and (F) cortex, in MS patients. The symbol (*) indicates phenotypes with a

significantly non-zero (i.e., healthy population expected value) mean estimated z-score, as well as significant between-group comparisons (linear models). FDR correction (Benjamini-Hochberg procedure) was applied. See main text and Table 5 for further details. Abbreviations: CIS=clinically isolated syndrome; MS=multiple sclerosis; NAWM=normal-appearing white matter; RRMS=relapsing-remitting multiple sclerosis; SPMS=secondary progressive multiple sclerosis; PPMS=primary progressive multiple sclerosis; T1w/T2w-ratio=T1weighted/T2weighted-ratio; WM=white matter.

Table 5. Mean estimated T1w/T2w-ratio z-scores in MS patients as a whole and according to their clinical phenotype in different brain compartments.

	MS		CIS		RRMS		SPMS		PPMS		
	Mean (SD)	**p (FDR p)**	**Mean (SD)**	**p (FDR p)**	**Mean (SD)**	**p (FDR p)**	**Mean (SD)**	**p (FDR p)**	**Mean (SD)**	**p (FDR p)**	**p[a]**
WM lesions	-4.531 (1.426)	**<0.001 (<0.001)**	-4.251 (1.768)	**<0.001 (<0.001)**	-4.406 (1.317)	**<0.001 (<0.001)**	-4.897 (1.257)[b]	**<0.001 (<0.001)**	-4.536 (1.582)	**<0.001 (<0.001)**	**0.010**
NAWM	-0.266 (1.220)	**0.001 (0.001)**	-0.152 (1.224)	0.351 (0.508)	-0.366 (1.148)	**0.001 (0.001)**	-0.314 (1.245)	**0.011 (0.026)**	-0.021 (1.343)	0.890 (0.920)	0.213
Thalamus	-0.001 (1.163)	0.989 (0.989)	-0.089 (1.094)	0.541 (0.701)	-0.041 (1.080)	0.598 (0.718)	-0.023 (1.237)	0.849 (0.906)	0.202 (1.308)	0.185 (0.355)	0.491
Striatum	0.349 (1.328)	**0.001 (0.001)**	0.040 (1.145)	0.792 (0.864)	0.201 (1.227)	**0.023 (0.042)**	0.555 (1.338)[c]	**0.001 (0.001)**	0.681 (1.588)	**0.001 (0.001)**	**0.008**
Pallidum	0.536 (1.367)	**<0.001 (<0.001)**	0.186 (1.240)	0.262 (0.393)	0.351 (1.318)	**0.001 (0.001)**	0.913 (1.333)[d]	**0.001 (0.001)**	0.754 (1.492)	**0.001 (0.001)**	**<0.001**
Cortex	-0.270 (1.246)	**0.001 (0.001)**	-0.173 (1.090)	0.237 (0.392)	-0.246 (1.158)	**0.003 (0.008)**	-0.430 (1.364)	**0.001 (0.004)**	-0.183 (1.401)	0.262 (0.393)	0.523

p values of the test for the nullity (i.e., healthy population expected value) of the mean estimated z-scores in each group and of significant between-group comparisons are reported (linear models). FDR correction (Benjamini-Hochberg procedure) was applied to account for the overall number of tests. Bold values denote statistical significance ($p<0.05$).

p[a]Heterogeneity among MS phenotypes.
[b,c,d]Significant SPMS vs RRMS post hoc comparisons: b) p (FDR p) = 0.002 (0.004); c) p (FDR p) = 0.025 (0.045); d) p (FDR p) = 0.001 (0.002).

Abbreviations: CIS=clinically isolated syndrome; FDR=false discovery rate; MS=multiple sclerosis; NAWM=normal-appearing white matter; PPMS=primary progressive multiple sclerosis; RRMS=relapsing-remitting multiple sclerosis; SPMS=secondary progressive multiple sclerosis; PPMS=primary progressive multiple sclerosis; WM=white matter.

4.4. T1w/T2w-ratio according to EDSS milestones

T1w/T2w-ratio z-scores in relapse- and progressive-onset MS patients according to EDSS milestones in different brain compartments are summarized in Table 6 and Figure 11.

In relapse-onset MS, compared to HC, T1w/T2w-ratio was significantly lower in WM lesions (all FDR $p<0.001$) and NAWM (FDR p ranging from 0.008 to 0.023) starting from mild disability (EDSS<3.0) and in the cortex starting from moderate disability (EDSS≥3.0) (FDR p ranging from 0.007 to 0.023). Conversely, T1w/T2w-ratio was significantly higher in the striatum and pallidum only from EDSS≥4.0 onward (FDR p ranging from 0.001 to 0.005).

In PPMS patients, T1w/T2w-ratio was significantly lower in WM lesions starting at EDSS<6.0 (FDR $p<0.001$) and significantly higher in the striatum and pallidum beyond EDSS≥6.0 (FDR $p=0.001$ and <0.001, respectively).

Between-group comparisons confirmed the described T1w/T2w-ratio behavior along increasing disability levels (see Table 6 and Figure 10).

Results did not change when adjusting for treatment. No influence of DMT on T1w/T2w-ratio within-group estimates ($p\geq0.069$) and between-group comparisons ($p\geq0.107$) was detected.

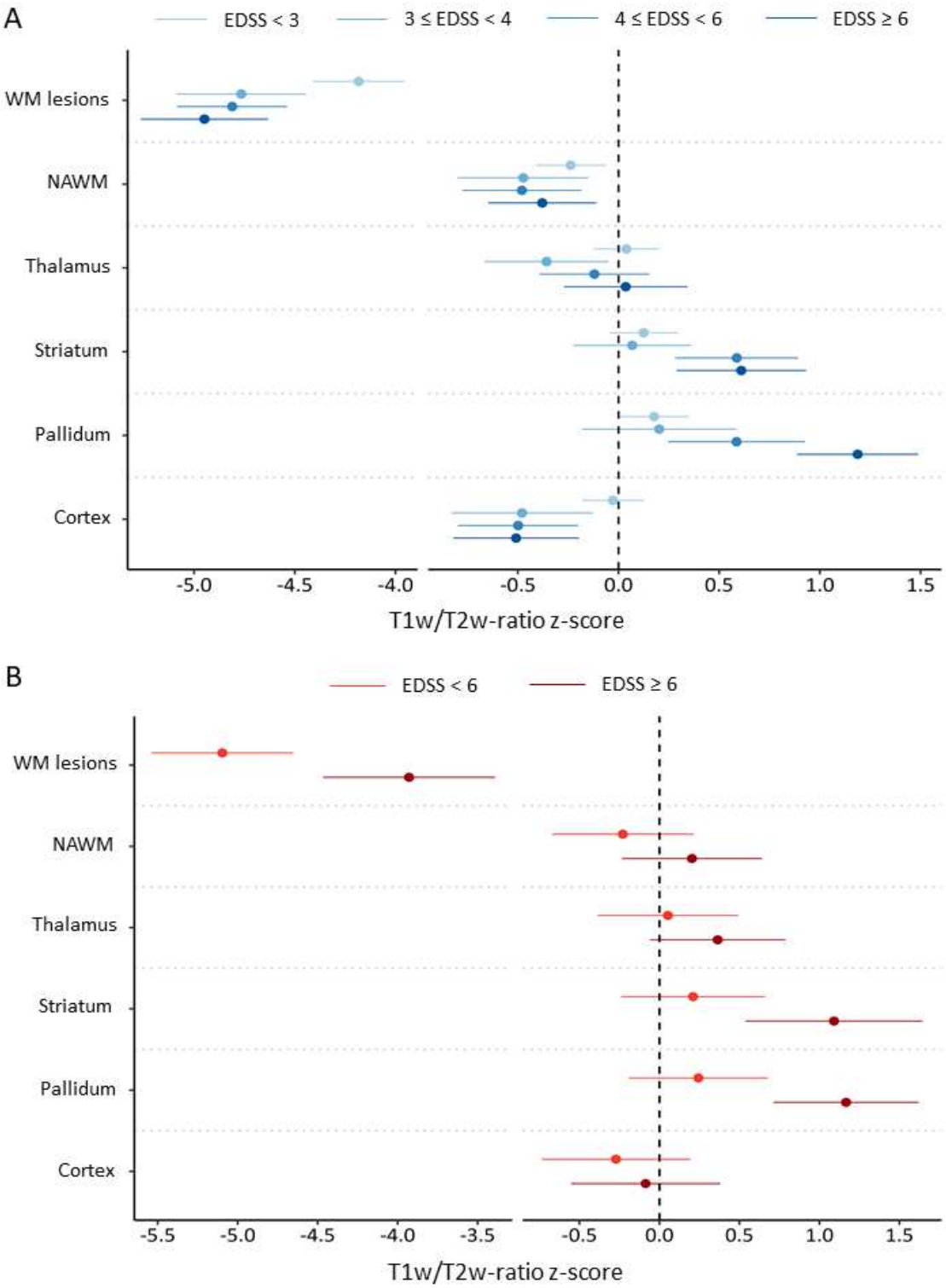

Figure 11. Mean estimated T1w/T2w-ratio *z*-scores in relapse- and progressive-onset MS patients according to EDSS milestones in different brain compartments.

T1w/T2w-ratio mean estimated *z*-scores with 95% confidence intervals in white matter lesions, normal-appearing white matter, thalamus, striatum, pallidum and cortex,

according to increasing disability levels**,** in (A) relapse-onset and (B) progressive-onset MS patients (linear models). See main text and Table 6 for further details.
Abbreviations: EDSS=Expanded disability status scale; NAWM=normal-appearing white matter; T1w/T2w-ratio=T1weighted/T2weighted-ratio; WM=white matter.

Table 6. Mean estimated T1w/T2w-ratio z-scores in relapse- and progressive-onset MS patients according to EDSS milestones in different brain compartments.

	Relapse-onset MS								Progressive-onset MS				
	EDSS < 3 (n=178)		3 ≤ EDSS < 4 (n=45)		4 ≤ EDSS < 6 (n=68)		EDSS ≥ 6 (n=68)			EDSS < 6 (n=39)		EDSS ≥ 6 (n=36)	
	Mean (SD)	p (FDR p)	Mean (SD)	p (FDR p)	Mean (SD)	p (FDR p)	Mean (SD)	p (FDR p)	p[a]	Mean (SD)	p (FDR p)	Mean (SD)	p (FDR p)	p[a]
WM lesions	-4.183 (1.514)	**<0.001 (<0.001)**	-4.766[b] (1.072)	**<0.001 (<0.001)**	-4.811[b] (1.127)	**<0.001 (<0.001)**	-4.949[b] (1.306)	**<0.001 (<0.001)**	**<0.001**	-5.096 (1.367)	**<0.001 (<0.001)**	-3.929[e] (1.592)	**<0.001 (<0.001)**	**0.001**
NAWM	-0.239 (1.185)	**0.008 (0.023)**	-0.473 (1.083)	**0.005 (0.019)**	-0.480 (1.224)	**0.002 (0.008)**	-0.379 (1.082)	**0.006 (0.020)**	0.408	-0.229 (1.366)	0.302 (0.422)	0.203 (1.298)	0.354 (0.425)	0.165
Thalamus	0.039 (1.095)	0.637 (0.800)	-0.357[b] (1.022)	**0.024 (0.049)**	-0.120 (1.123)	0.382 (0.551)	0.036 (1.266)	0.817 (0.942)	0.130	0.053 1.356)	0.809 (0.809)	0.364 (1.252)	0.090 (0.202)	0.305
Striatum	0.125 (1.131)	0.147 (0.253)	0.068 (0.964)	0.643 (0.800)	0.587[b,c] (1.222)	**<0.001 (0.002)**	0.610[b,c] (1.331)	**<0.001 (0.002)**	**0.005**	0.210 (1.363)	0.348 (0.425)	1.091[e] (1.634)	**<0.001 (0.001)**	**0.014**
Pallidum	0.177 (1.143)	0.044 (0.082)	0.202 (1.273)	0.293 (0.451)	0.586 (1.405)	**0.001 (0.005)**	1.188[b,c,d] (1.240)	**<0.001 (<0.001)**	**<0.001**	0.243 (1.323)	0.264 (0.422)	1.167[e] (1.34)	**<0.001 (<0.001)**	**0.004**
Cortex	-0.028 (1.024)	0.723 (0.866)	-0.479[b] (1.166)	**0.008 (0.023)**	-0.499[b] (1.234)	**0.001 (0.007)**	-0.509[b] (1.269)	**0.002 (0.008)**	**0.003**	-0.272 (1.432)	0.244 (0.422)	-0.087 (1.379)	0.709 (0.750)	0.570

p values of the test for the nullity (i.e., healthy population expected value) of the mean estimated z-scores in each group and of significant between-group comparisons are reported (linear models). FDR correction (Benjamini-Hochberg procedure) was applied to account for the overall number of tests. Bold values denote statistical significance ($p<0.05$).

p[a]Heterogeneity among MS patients' groups, classified according to EDSS milestones.
[b]Significant post hoc comparisons vs EDSS<3 (FDR p range: <0.001-0.021; FDR p range: <0.001-0.045).
[c]Significant post hoc comparisons vs 3≤ EDSS<4 (FDR p range: <0.001-0.015; FDR p range: <0.001-0.034).
[d]Significant post hoc comparisons vs 4≤ EDSS<6 (FDR p=0.009; FDR p=0.023).
[e]Significant post hoc comparisons vs EDSS<6 (FDR p range: 0.001-0.014; FDR p range: 0.004-0.037).

Abbreviations: CIS=clinically isolated syndrome; EDSS=Expanded Disability Status Scale; FDR=false discovery rate; MS=multiple sclerosis; NAWM=normal-appearing white matter; WM=white matter.

4.5. Analysis of associations

Associations between clinical and MRI variables with T1w/T2w-ratio in MS patients are summarized in Table 7.

A longer disease duration, higher EDSS score, higher brain T2-hyperintense WM LV, and a lower NBV were significantly associated with a lower T1w/T2w-ratio in T2-hyperintense WM lesions (ß ranging from -1.168 to 0.005, FDR p ranging from <0.001 to 0.011) and with a higher T1w/T2w-ratio in the pallidum and striatum (ß ranging from to -0.005 to 0.286, FDR p ranging from <0.001 to 0.040). A longer disease duration was also significantly associated with a lower cortical T1w/T2w-ratio (ß=-0.014, FDR p=0.036), whereas a higher brain T2-hyperintense WM LV was associated with a lower T1w/T2w-ratio both in the cortex and NAWM (ß=-0.313, FDR p=0.010 and ß =-0.442, FDR p<0.001).

Results did not change when adjusting for treatment. No significant interaction effects on the associations due to DMT were detected (p≥0.102), with no effect on the differences of association between relapse-onset and progressive-onset disease course (p>0.118).

Table 7. Associations between disease duration, Expanded Disability Status Scale (EDSS) score, brain T2 lesion volume (LV) and NBV (normalized brain volume) with T1w/T2w-ratio z-scores in multiple sclerosis patients as a whole, and classified in relapse- and progressive-onset patients, in different brain compartments.

		MS		**Relapse-onset MS**		**Progressive-onset MS**		**Progressive- vs relapse-onset MS**
		β (SE)	**p (FDR p)**	**β (SE)**	**p (FDR p)**	**β (SE)**	**p (FDR p)**	**p (FDR p)**
WM lesions T1w/T2w-ratio	Disease duration	-0.027 (0.007)	**<0.001 (<0.001)**	-0.036 (0.007)	**<0.001 (<0.001)**	0.020 (0.019)	0.287 (0.412)	**0.005 (0.016)**
	EDSS	-0.095 (0.032)	**0.003 (0.011)**	-0.152 (0.035)	**<0.001 (<0.001)**	0.278 (0.120)	0.021 (0.050)	**<0.001 (0.003)**
	Brain T2 LV	-1.168 (0.108)	**<0.001 (<0.001)**	-1.072 (0.115)	**<0.001 (<0.001)**	-1.772 (0.275)	**<0.001 (<0.001)**	0.020 (0.050)
	NBV	0.005 (0.001)	**<0.001 (<0.001)**	0.005 (0.001)	**<0.001 (<0.001)**	0.006 (0.003)	0.038 (0.081)	0.767 (0.817)
NAWM T1w/T2w-ratio	Disease duration	-0.005 (0.006)	0.377 (0.490)	-0.008 (0.006)	0.167 (0.272)	0.022 (0.016)	0.175 (0.275)	0.080 (0.151)
	EDSS	0.022 (0.028)	0.431 (0.531)	-0.02 (0.0300)	0.504 (0.598)	0.178 (0.103)	0.086 (0.159)	0.066 (0.130)
	Brain T2 LV	-0.442 (0.105)	**<0.001 (<0.001)**	-0.422 (0.111)	**<0.001 (<0.001)**	-0.741 (0.290)	**0.013 (0.036)**	0.304 (0.420)
	NBV	0.001 (0.001)	0.559 (0.632)	0.001 (0.001)	0.265 (0.391)	-0.001 (0.002)	0.624 (0.678)	0.395 (0.500)
Thalamic T1w/T2w-ratio	Disease duration	-0.004 (0.005)	0.405 (0.505)	-0.006 (0.006)	0.304 (0.420)	0.010 (0.016)	0.518 (0.606)	0.337 (0.456)
	EDSS	0.036 (0.026)	0.172 (0.275)	0.006 (0.029)	0.839 (0.852)	0.181 (0.100)	0.072 (0.139)	0.095 (0.168)
	Brain T2 LV	-0.115 (0.103)	0.269 (0.391)	-0.093 (0.109)	0.396 (0.500)	-0.370 (0.290)	0.206 (0.315)	0.372 (0.490)
	NBV	-0.001 (0.001)	0.239 (0.358)	-0.001 (0.001)	0.306 (0. 420)	0.001 (0.002)	0.843 (0.852)	0.871 (0.871)

	Disease duration	0.017 (0.006)	**0.005 (0.014)**	0.012 (0.006)	0.045 (0.092)	0.053 (0.018)	**0.003 (0.010)**	0.031 (0.068)
Striatum T1w/T2w-ratio	EDSS	0.149 (0.028)	**<0.001 (<0.001)**	0.122 (0.030)	**<0.001 (<0.001)**	0.377 (0.114)	**0.001 (0.004)**	0.031 (0.068)
	Brain T2 LV	0.259 (0.112)	0.022 (0.051)	0.261 (0.115)	0.024 (0.055)	0.083 (0.350)	0.814 (0.845)	0.628 (0.678)
	NBV	-0.004 (0.001)	**<0.001 (<0.001)**	-0.004 (0.001)	**<0.001 (<0.001)**	-0.006 (0.003)	0.043 (0.091)	0.555 (0.632)
	Disease duration	0.026 (0.006)	**<0.001 (<0.001)**	0.024 (0.006)	**<0.001 (0.001)**	0.048 (0.016)	**0.003 (0.010)**	0.165 (0.272)
Pallidum T1w/T2w-ratio	EDSS	0.199 (0.028)	**<0.001 (<0.001)**	0.196 (0.032)	**<0.001 (<0.001)**	0.361 (0.102)	**<0.001 (0.002)**	0.123 (0.207)
	Brain T2 LV	0.286 (0.117)	**0.015 (0.040)**	0.303 (0.125)	**0.016 (0.042)**	0.073 (0.316)	0.819 (0.845)	0.498 (0.598)
	NBV	-0.005 (0.001)	**<0.001 (<0.001)**	-0.005 (0.001)	**<0.001 (<0.001)**	-0.003 (0.003)	0.190 (0.294)	0.593 (0.655)
	Disease duration	-0.014 (0.006)	**0.013 (0.036)**	-0.018 (0.006)	**0.002 (0.007)**	0.012 (0.017)	0.489 (0.594)	0.092 (0.166)
Cortical T1w/T2w-ratio	EDSS	-0.053 (0.028)	0.054 (0.108)	-0.087 (0.03)	**0.004 (0.012)**	0.097 (0.109)	0.377 (0.490)	0.105 (0.183)
	Brain T2 LV	-0.313 (0.104)	**0.003 (0.010)**	-0.298 (0.110)	**0.007 (0.022)**	-0.479 (0.295)	0.109 (0.187)	0.566 (0.632)
	NBV	0.002 (0.001)	0.020 (0.050)	0.002 (0.001)	**0.014 (0.040)**	0.001 (0.002)	0.564 (0.632)	0.775 (0.817)

Beta coefficients (β) and p values from linear models are reported. FDR correction (Benjamini-Hochberg procedure) was applied to account for the overall number of tests. Bold values denote statistical significance ($p<0.05$).

Abbreviations: EDSS=Expanded Disability Status Scale; FDR=false discovery rate; LV=lesion volume; MS=multiple sclerosis; NAWM=normal-appearing white matter; NBV=normalized brain volume; SE=standard error; WM=white matter.

5. DISCUSSION

In this study, we evaluated T1w/T2w-ratio in the different brain compartments in a large multicenter cohort of HC and MS patients including the main disease clinical phenotypes. This allowed us to obtain relevant information regarding the trajectories of T1w/T2w-ratio occurring with aging and how clinical phenotypes, severity of disability and structural brain damage accumulation are associated with brain T1w/T2w-ratio abnormalities in MS patients.

In HC, we found that T1w/T2w-ratio increased over time, reaching a plateau around 50-60 years of age for all the brain compartments, suggesting that, in addition to myelin density, other substrates may contribute to maturational and aging processes. In MS patients, heterogeneous T1w/T2w-ratio alterations were detected in specific brain compartments according to disease clinical phenotypes and levels of disability. In particular, compared to HC, T1w/T2w-ratio was lower in T2-hyperintense WM lesions and NAWM already from the earliest phases of the disease and from mild levels of disability, whereas a lower cortical T1w/T2w-ratio was detected only in RRMS and SPMS patients and beyond accrual of moderate levels of disability. Interestingly, a significant higher T1w/T2w-ratio was found in the striatum and pallidum especially in patients with PMS and more severe disability; thalamic values were intermediate and did not change much.

5.1. T1w/T2w-ratio in normal brain aging

In line with previous studies,[176, 177] the analysis on HC showed that T1w/T2w-ratio varied across the adult lifespan in the different brain compartments. In particular, T1w/T2w-ratio gradually increased until mid-age, followed by a plateau in all the investigated structures. Of note, in the deep GM nuclei, especially in the pallidum and striatum, a steeper increase occurred in the first decades. Different physiological processes may explain our findings. T1w/T2w-ratio has been suggested to be associated with myelin density.[137] Accordingly, the process of brain myelination may contribute to the increase of T1w/T2w-ratio at least in the first decades of life.[178-181] Since iron influences both signal on T1- and T2w images[144, 182] and it co-localizes with myelin in the cortex and WM,[142, 182, 183] it may also contribute, together with myelin

macromolecules, to T1w/T2w-ratio values.[144] In T2 spin echo sequences, the effect of iron in reducing T2 relaxation time is related to water diffusivity. Specifically, it is evident when the diffusion distance and the size of the cells (where iron is presumably compartmentalized) are comparable in terms of diameter.[184, 185] Considering the relatively low myelin content within the deep GM nuclei (except for the thalamus and globus pallidus),[186, 187] the observed trajectories support the contribution of iron and neurodegeneration in determining the increase of T1w/T2w-ratio with healthy aging.[188, 189] When myelination is accomplished, there is no further iron accumulation in oligodendrocytes.[182, 190] However, microglia and astrocytes continue to accumulate iron during adulthood and senescence,[190, 191] possibly explaining the high iron levels found in the basal ganglia in post-mortem studies,[182, 188, 192] and the age-related increase of susceptibility on quantitative susceptibility mapping studies.[193-195]

5.2. T1w/T2w-ratio in multiple sclerosis brain

The most relevant results are those we obtained from the evaluation of T1w/T2w-ratio in the different brain compartments of MS patients according to their disease severity.

In line with a previous study,[164] we found a significantly lower T1w/T2w-ratio in T2-hyperintense WM lesions in all the clinical phenotypes and already from mild disability. According to histopathological studies,[124, 196] demyelination, axonal damage and loss of iron may explain our findings (Figure 12). Interestingly, more severe damage was found in patients with SPMS and more severe disability. Our findings suggest that, although the pathological processes occurring in focal WM lesions are similar across the MS spectrum, a more severe disease is characterized by more relevant lesional microstructural abnormalities.[197, 198]

In the NAWM, compared to HC, T1w/T2w-ratio was significantly lower already from mild disability levels and in RRMS and SPMS patients, but not in those with CIS and PPMS. Although in contrast with some previous reports,[159, 164] our results in RRMS patients are consistent with other studies,[160-162, 166] showing no significant differences in the early phases of the disease but only in patients with a longer disease duration. Discrepancies among studies may be explained by heterogeneities in the cohorts of MS patients investigated, often with small sample sizes and short disease duration, and in the

methods applied to quantify T1w/T2w-ratio. Despite this, our results further confirm that NAWM is characterized by the occurrence of microstructural abnormalities, with inflammation, demyelination, gliosis and axonal damage (Figure 12),[21] already from the early phases of the disease, as already shown by previous DT imaging[199, 200] and MT MRI[201-204] studies.

In line with previous studies,[148, 165] compared to HC, cortical T1w/T2w-ratio was significantly lower from moderate levels of disability and in RRMS and SPMS patients, but not in those with CIS and PPMS. Although we did not evaluate cortical lesions, our findings further support the role of cortical involvement in determining clinical disability.[205, 206]

Unexpectedly, we found no differences in NAWM and cortical T1w/T2w-ratio between PPMS patients and HC nor a significant decline in SPMS compared to RRMS patients.

MS patients with a progressive disease course and more severe disability are characterized by a progressive reduction of myelin and oligodendrocytes, typically rich of iron, thus promoting a further decline of T1w/T2w-ratio in the NAWM and cortex. However, age-related physiological iron increase in oligodendrocytes and myelin may act in the opposite direction (Figure 12).[27, 207] Moreover, a more substantial microglia activation and astrogliosis with a patchy iron redistribution, especially in PMS patients, may also contribute to explain our findings.[21, 192]

The most complex results of our work came from the assessment of deep GM nuclei of MS patients, where T1w/T2w-ratio showed an opposite behavior compared to the other brain compartments. Compared to HC, T1w/T2w-ratio in the pallidum and striatum was significantly higher from moderate levels of disability and in all disease clinical phenotypes, except for patients with CIS. Of note, the highest T1w/T2w-ratio values were found in SPMS and PPMS patients. Our findings are consistent with previous studies that evaluated T1w/T2w-ratio in other neurodegenerative diseases.[151, 152, 208, 209] Patients with Parkinson disease showed higher T1w/T2w-ratio in the substantia nigra.[152] In Alzheimer disease,[151] Huntington disease[208] and multiple system atrophy,[209] cortical and WM T1w/T2w-ratio, respectively, were significantly higher compared to HC. Our results in the pallidum and striatum, together with the demonstration of significantly higher T1w/T2w-ratio in brain regions, known to be specifically affected by other

diseases, suggest that T1w/T2w-ratio may reflect ongoing neurodegenerative processes (Figure 12).

Interestingly and differently from the other deep GM nuclei, we found no significant alterations of T1w/T2w-ratio values in the thalamus in MS patients, independently from the clinical phenotype and clinical disability. Heterogeneous pathological processes including demyelination, microglia activation, neuronal loss and iron accumulation may affect the thalamus in MS and may influence T1w/T2w-ratio in opposite ways.[210-212] Of note, discordant evidence exists regarding thalamic iron concentration in this condition, with the majority of pathological and MRI studies suggesting no differences in thalamic iron content compared to HC,[194, 211, 213] not confirmed by others showing decreased iron.[186, 214] The peculiar morphological architecture of the thalamus, characterized by more abundant WM fibers and iron-rich oligodendrocytes compared with other structures (i.e., pallidum, striatum) likely contribute to explain our findings in this nucleus.[192]

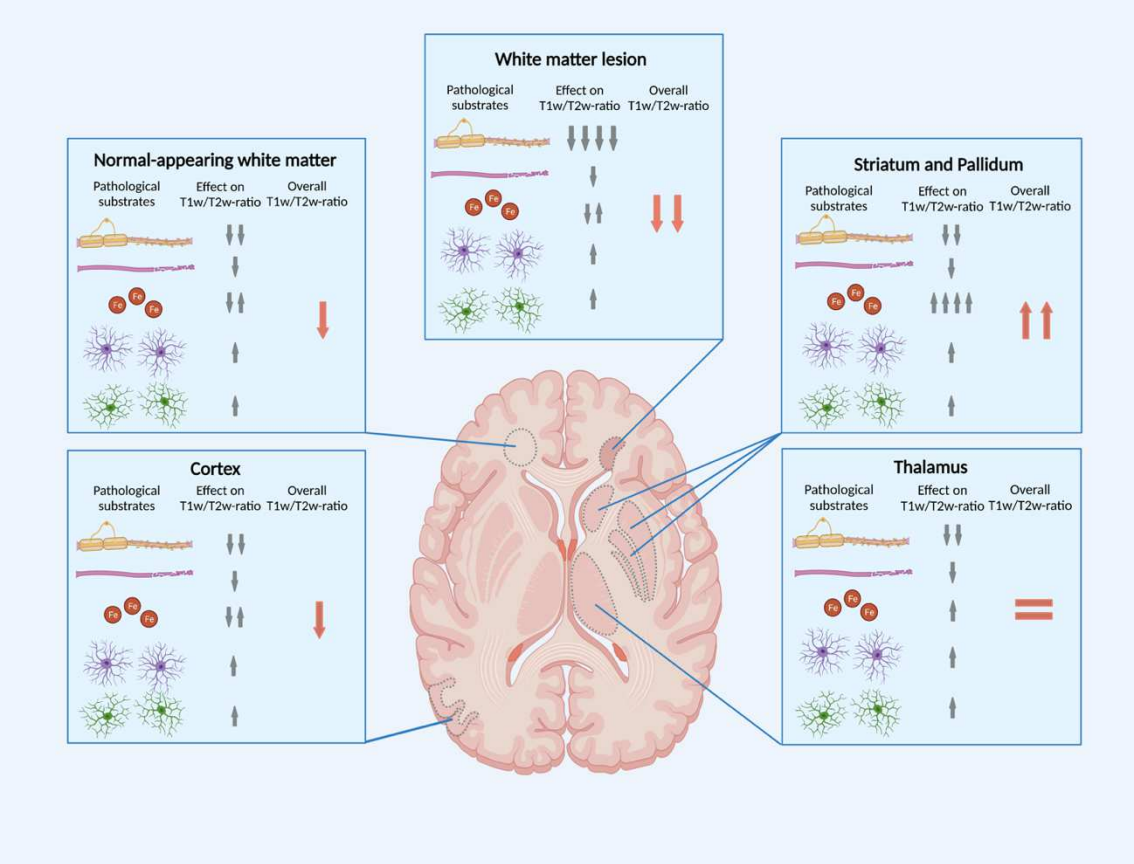

Figure 12. Overview of the different pathological substrates of MS and their possible effects on T1w/T2w-ratio.

The pathological mechanisms involved in MS may influence T1w/T2w-ratio with opposite behaviors and heterogeneously in the different brain compartments investigated in the study. Demyelination/inflammation (yellow) and axonal damage (pink) are likely to reduce T1w/T2w-ratio; conversely, iron accumulation (red), microglia activation (violet) and astrogliosis (green) may increase T1w/T2w-ratio. In T2-hyperintense WM lesions, NAWM and cortex, the effects of demyelination/inflammation and axonal damage on T1w/T2w-ratio are likely to be more prominent than those of iron accumulation (red), microglia activation (violet) and astrogliosis (green), thus promoting an overall reduction of T1w/T2w-ratio. On the other hand, in the striatum and pallidum, the effects of microglia activation (violet) and astrogliosis (green), and, above all, iron accumulation (red) are likely to be more prominent, thus resulting in an overall increase of T1w/T2w-ratio. In the thalamus, the effects of the different pathological processes counteract each other, thus nullifying differences in T1w/T2w-ratio. Created with biorender.com.

Abbreviations: MS=multiple sclerosis; NAWM=normal-appearing white matter; T1w/T2w-ratio=T1weighted/T2weighted ratio; WM=white matter.

5.3. Associations with clinical and MRI parameters

Regarding the clinical relevance of this metric, differently from previous studies,[148, 160] the significant associations found between both EDSS score and disease duration with T1w/T2w ratio in T2-hyperintense WM lesion, cortex, striatum, and pallidum, suggest a gradual and progressive accumulation of clinically relevant microstructural tissue abnormalities in the different brain compartments.

The significant associations between higher brain T2-hyperintense WM LV and lower T1w/T2w-ratio in the NAWM and cortex and higher T1w/T2w-ratio in the pallidum and striatum suggest that diffuse abnormalities may be, at least partially, secondary to retrograde degeneration due to the accumulation of focal demyelinating T2-hyperintense lesions in the WM. Moreover, the associations with brain volume also suggested the relevance of T1w/T2w-ratio values as a surrogate measure of irreversible tissue loss.

5.4. Limitations

This study has some limitations. First, we evaluated T1w/T2w-ratio as a global measure in all the investigated brain compartments with a cross-sectional approach. Since different regions are characterized by specific cyto-architectural features and MS may affect the different regions with spatial and temporal heterogeneities, future studies are needed to better evaluate MS pathology at a regional level and in a longitudinal setting to explore the dynamic patterns of T1w/T2w-ratio and their associations with disease progression. Second, we did not evaluate cortical lesions, thus the results found for cortical T1w/T2w-ratio may be influenced, at least partially, by focal cortical demyelination.

Third, the observed T1w/T2w-ratio values showed a relatively high variability, possibly related also to the multicenter design. Indeed, even though the proposed method uses a calibration to reduce the intensity variability, different scans and sequences were used. However, appropriate adjustments for site were included in the statistical models to provide site-specific T1w/T2w-ratio z-scores that were used in subsequent statistical analyses. Finally, MS patients were older than HC, thus requiring statistical age adjustment.

6. CONCLUSIONS

In summary, in HC we demonstrated an increase of T1w/T2w-ratio with age in all the investigated brain compartments. In MS patients, we observed lower T1w/T2w-ratio values in T2-hyperintense WM lesions and NAWM already from the earliest phases of the disease and from mild levels of disability, whereas a lower cortical T1w/T2w-ratio was detected only in RRMS and SPMS patients and beyond accrual of moderate levels of disability. Conversely, higher T1w/T2w-ratio was found in the striatum and pallidum especially in patients with PMS and more severe disability. Altogether, our data suggest that T1w/T2w-ratio results from several pathological substrates, including inflammation, demyelination, neurodegeneration and iron accumulation. Given its broad availability, the T1w/T2w-ratio may represent a clinically relevant method to investigate *in vivo* the heterogeneous processes affecting the brain of MS patients.

7. REFERENCES

1. Filippi M, Bar-Or A, Piehl F, et al. Multiple sclerosis. Nat Rev Dis Primers 2018;4:43.
2. Lublin FD, Reingold SC, Cohen JA, et al. Defining the clinical course of multiple sclerosis: the 2013 revisions. Neurology 2014;83:278-286.
3. Geraldes R, Ciccarelli O, Barkhof F, et al. The current role of MRI in differentiating multiple sclerosis from its imaging mimics. Nat Rev Neurol 2018.
4. Thompson AJ, Banwell BL, Barkhof F, et al. Diagnosis of multiple sclerosis: 2017 revisions of the McDonald criteria. Lancet Neurol 2018;17:162-173.
5. Collaborators GBDMS. Global, regional, and national burden of multiple sclerosis 1990-2016: a systematic analysis for the Global Burden of Disease Study 2016. Lancet Neurol 2019;18:269-285.
6. Yeshokumar AK, Narula S, Banwell B. Pediatric multiple sclerosis. Curr Opin Neurol 2017;30:216-221.
7. Tremlett H, Devonshire V. Is late-onset multiple sclerosis associated with a worse outcome? Neurology 2006;67:954-959.
8. Koch-Henriksen N, Sorensen PS. The changing demographic pattern of multiple sclerosis epidemiology. Lancet Neurol 2010;9:520-532.
9. Orton SM, Herrera BM, Yee IM, et al. Sex ratio of multiple sclerosis in Canada: a longitudinal study. Lancet Neurol 2006;5:932-936.
10. Olsson T, Barcellos LF, Alfredsson L. Interactions between genetic, lifestyle and environmental risk factors for multiple sclerosis. Nat Rev Neurol 2017;13:25-36.
11. Amato MP, Derfuss T, Hemmer B, et al. Environmental modifiable risk factors for multiple sclerosis: Report from the 2016 ECTRIMS focused workshop. Mult Scler 2017:1352458516686847.
12. Endriz J, Ho PP, Steinman L. Time correlation between mononucleosis and initial symptoms of MS. Neurol Neuroimmunol Neuroinflamm 2017;4:e308.
13. Lai YH, Fang TC. The pleiotropic effect of vitamin d. ISRN Nephrol 2013;2013:898125.
14. Pierrot-Deseilligny C, Souberbielle JC. Vitamin D and multiple sclerosis: An update. Mult Scler Relat Disord 2017;14:35-45.

15. Handel AE, Williamson AJ, Disanto G, Dobson R, Giovannoni G, Ramagopalan SV. Smoking and multiple sclerosis: an updated meta-analysis. PLoS One 2011;6:e16149.
16. Hindson J. Multiple sclerosis: A possible link between multiple sclerosis and gut microbiota. Nat Rev Neurol 2017;13:705.
17. Harirchian MH, Fatehi F, Sarraf P, Honarvar NM, Bitarafan S. Worldwide prevalence of familial multiple sclerosis: A systematic review and meta-analysis. Mult Scler Relat Disord 2017;20:43-47.
18. Compston A, Coles A. Multiple sclerosis. Lancet 2002;359:1221-1231.
19. Baranzini SE, Oksenberg JR. The Genetics of Multiple Sclerosis: From 0 to 200 in 50 Years. Trends Genet 2017;33:960-970.
20. Lucchinetti C, Bruck W, Parisi J, Scheithauer B, Rodriguez M, Lassmann H. Heterogeneity of multiple sclerosis lesions: implications for the pathogenesis of demyelination. Ann Neurol 2000;47:707-717.
21. Kutzelnigg A, Lucchinetti CF, Stadelmann C, et al. Cortical demyelination and diffuse white matter injury in multiple sclerosis. Brain 2005;128:2705-2712.
22. Green AJ, McQuaid S, Hauser SL, Allen IV, Lyness R. Ocular pathology in multiple sclerosis: retinal atrophy and inflammation irrespective of disease duration. Brain 2010;133:1591-1601.
23. Gilmore CP, Donaldson I, Bo L, Owens T, Lowe J, Evangelou N. Regional variations in the extent and pattern of grey matter demyelination in multiple sclerosis: a comparison between the cerebral cortex, cerebellar cortex, deep grey matter nuclei and the spinal cord. J Neurol Neurosurg Psychiatry 2009;80:182-187.
24. Frischer JM, Weigand SD, Guo Y, et al. Clinical and pathological insights into the dynamic nature of the white matter multiple sclerosis plaque. Ann Neurol 2015;78:710-721.
25. Machado-Santos J, Saji E, Troscher AR, et al. The compartmentalized inflammatory response in the multiple sclerosis brain is composed of tissue-resident CD8+ T lymphocytes and B cells. Brain 2018;141:2066-2082.
26. Lassmann H, van Horssen J, Mahad D. Progressive multiple sclerosis: pathology and pathogenesis. Nat Rev Neurol 2012;8:647-656.

27. Mahad DH, Trapp BD, Lassmann H. Pathological mechanisms in progressive multiple sclerosis. Lancet Neurol 2015;14:183-193.
28. Prineas JW, Kwon EE, Cho ES, et al. Immunopathology of secondary-progressive multiple sclerosis. Ann Neurol 2001;50:646-657.
29. Luchetti S, Fransen NL, van Eden CG, Ramaglia V, Mason M, Huitinga I. Progressive multiple sclerosis patients show substantial lesion activity that correlates with clinical disease severity and sex: a retrospective autopsy cohort analysis. Acta Neuropathol 2018;135:511-528.
30. Dendrou CA, Fugger L, Friese MA. Immunopathology of multiple sclerosis. Nat Rev Immunol 2015;15:545-558.
31. Dal-Bianco A, Grabner G, Kronnerwetter C, et al. Slow expansion of multiple sclerosis iron rim lesions: pathology and 7 T magnetic resonance imaging. Acta Neuropathol 2017;133:25-42.
32. Staffen W, Zauner H, Mair A, et al. Magnetic resonance spectroscopy of memory and frontal brain region in early multiple sclerosis. J Neuropsychiatry Clin Neurosci 2005;17:357-363.
33. Calabrese M, Magliozzi R, Ciccarelli O, Geurts JJ, Reynolds R, Martin R. Exploring the origins of grey matter damage in multiple sclerosis. Nat Rev Neurosci 2015;16:147-158.
34. Filippi M, Bruck W, Chard D, et al. Association between pathological and MRI findings in multiple sclerosis. Lancet Neurol 2019;18:198-210.
35. Albert M, Antel J, Bruck W, Stadelmann C. Extensive cortical remyelination in patients with chronic multiple sclerosis. Brain Pathol 2007;17:129-138.
36. Strijbis EMM, Kooi EJ, van der Valk P, Geurts JJG. Cortical Remyelination Is Heterogeneous in Multiple Sclerosis. J Neuropathol Exp Neurol 2017;76:390-401.
37. Patrikios P, Stadelmann C, Kutzelnigg A, et al. Remyelination is extensive in a subset of multiple sclerosis patients. Brain 2006;129:3165-3172.
38. Harlow DE, Honce JM, Miravalle AA. Remyelination Therapy in Multiple Sclerosis. Front Neurol 2015;6:257.
39. Prineas JW, Barnard RO, Kwon EE, Sharer LR, Cho ES. Multiple sclerosis: remyelination of nascent lesions. Ann Neurol 1993;33:137-151.

40. Franklin RJ, Ffrench-Constant C. Remyelination in the CNS: from biology to therapy. Nat Rev Neurosci 2008;9:839-855.
41. Lassmann H. Multiple Sclerosis Pathology. Cold Spring Harb Perspect Med 2018;8.
42. Goldschmidt T, Antel J, Konig FB, Bruck W, Kuhlmann T. Remyelination capacity of the MS brain decreases with disease chronicity. Neurology 2009;72:1914-1921.
43. Li R, Patterson K, Bar-Or A. Reassessing the contributions of B cells in multiple sclerosis. Nat Rev Immunol 2018.
44. Lassmann H. Targets of therapy in progressive MS. Mult Scler 2017;23:1593-1599.
45. Dutta R, Trapp BD. Relapsing and progressive forms of multiple sclerosis: insights from pathology. Curr Opin Neurol 2014;27:271-278.
46. Miller D, Barkhof F, Montalban X, Thompson A, Filippi M. Clinically isolated syndromes suggestive of multiple sclerosis, part I: natural history, pathogenesis, diagnosis, and prognosis. Lancet Neurol 2005;4:281-288.
47. Miller DH, Chard DT, Ciccarelli O. Clinically isolated syndromes. Lancet Neurol 2012;11:157-169.
48. McAlpine D. Multiple sclerosis: a review. Br Med J 1973;2:292-295.
49. McDonald WI. Relapse, remission, and progression in multiple sclerosis. N Engl J Med 2000;343:1486-1487.
50. Vollmer T. The natural history of relapses in multiple sclerosis. J Neurol Sci 2007;256 Suppl 1:S5-13.
51. Toosy AT, Mason DF, Miller DH. Optic neuritis. Lancet Neurol 2014;13:83-99.
52. Petzold A, Wattjes MP, Costello F, et al. The investigation of acute optic neuritis: a review and proposed protocol. Nat Rev Neurol 2014;10:447-458.
53. Galetta SL, Villoslada P, Levin N, et al. Acute optic neuritis: Unmet clinical needs and model for new therapies. Neurol Neuroimmunol Neuroinflamm 2015;2:e135.
54. Rae-Grant AD, Eckert NJ, Bartz S, Reed JF. Sensory symptoms of multiple sclerosis: a hidden reservoir of morbidity. Mult Scler 1999;5:179-183.
55. McAlpine D. Symptoms and signs. In McApline D, Lumsden CE, Acheson ED, eds. Multiple Sclerosis: A Reappreaisal. Baltimore: Williams and Wilkins. 1972:132-196.

56. Dillon BE, Lemack GE. Urodynamics in the evaluation of the patient with multiple sclerosis: when are they helpful and how do we use them? Urol Clin North Am 2014;41:439-444, ix.
57. Rocca MA, Amato MP, De Stefano N, et al. Clinical and imaging assessment of cognitive dysfunction in multiple sclerosis. Lancet Neurol 2015;14:302-317.
58. Filippi M, Preziosa P, Rocca MA. Brain mapping in multiple sclerosis: Lessons learned about the human brain. NeuroImage 2019;190:32-45.
59. Feinstein A, Magalhaes S, Richard JF, Audet B, Moore C. The link between multiple sclerosis and depression. Nat Rev Neurol 2014;10:507-517.
60. Solaro C, Brichetto G, Amato MP, et al. The prevalence of pain in multiple sclerosis: a multicenter cross-sectional study. Neurology 2004;63:919-921.
61. Lublin FD, Reingold SC. Defining the clinical course of multiple sclerosis: results of an international survey. National Multiple Sclerosis Society (USA) Advisory Committee on Clinical Trials of New Agents in Multiple Sclerosis. Neurology 1996;46:907-911.
62. Confavreux C, Vukusic S. Natural history of multiple sclerosis: a unifying concept. Brain 2006;129:606-616.
63. Filippi M, Preziosa P, Banwell BL, et al. Assessment of lesions on magnetic resonance imaging in multiple sclerosis: practical guidelines. Brain 2019.
64. Rovira A, Wattjes MP, Tintore M, et al. Evidence-based guidelines: MAGNIMS consensus guidelines on the use of MRI in multiple sclerosis-clinical implementation in the diagnostic process. Nat Rev Neurol 2015;11:471-482.
65. Traboulsee A, Simon JH, Stone L, et al. Revised Recommendations of the Consortium of MS Centers Task Force for a Standardized MRI Protocol and Clinical Guidelines for the Diagnosis and Follow-Up of Multiple Sclerosis. AJNR Am J Neuroradiol 2016;37:394-401.
66. Dobson R, Ramagopalan S, Davis A, Giovannoni G. Cerebrospinal fluid oligoclonal bands in multiple sclerosis and clinically isolated syndromes: a meta-analysis of prevalence, prognosis and effect of latitude. J Neurol Neurosurg Psychiatry 2013;84:909-914.
67. Arrambide G, Tintore M, Espejo C, et al. The value of oligoclonal bands in the multiple sclerosis diagnostic criteria. Brain 2018;141:1075-1084.

68. Kuhle J, Disanto G, Dobson R, et al. Conversion from clinically isolated syndrome to multiple sclerosis: A large multicentre study. Mult Scler 2015;21:1013-1024.
69. Leocani L, Rocca MA, Comi G. MRI and neurophysiological measures to predict course, disability and treatment response in multiple sclerosis. Curr Opin Neurol 2016;29:243-253.
70. Charil A, Yousry TA, Rovaris M, et al. MRI and the diagnosis of multiple sclerosis: expanding the concept of "no better explanation". Lancet Neurol 2006;5:841-852.
71. Miller DH, Weinshenker BG, Filippi M, et al. Differential diagnosis of suspected multiple sclerosis: a consensus approach. Mult Scler 2008;14:1157-1174.
72. Schumacher F. Problems of experimental trials of therapy in multiple sclerosis. Ann N Y Acad Sci 1965;122:552-568.
73. Poser CM, Paty DW, Scheinberg L, et al. New diagnostic criteria for multiple sclerosis: guidelines for research protocols. Ann Neurol 1983;13:227-231.
74. McDonald WI, Compston A, Edan G, et al. Recommended diagnostic criteria for multiple sclerosis: guidelines from the International Panel on the diagnosis of multiple sclerosis. Ann Neurol 2001;50:121-127.
75. Polman CH, Reingold SC, Edan G, et al. Diagnostic criteria for multiple sclerosis: 2005 revisions to the "McDonald Criteria". Ann Neurol 2005;58:840-846.
76. Polman CH, Reingold SC, Banwell B, et al. Diagnostic criteria for multiple sclerosis: 2010 revisions to the McDonald criteria. Ann Neurol 2011;69:292-302.
77. van der Vuurst de Vries RM, Mescheriakova JY, Wong YYM, et al. Application of the 2017 Revised McDonald Criteria for Multiple Sclerosis to Patients With a Typical Clinically Isolated Syndrome. JAMA Neurol 2018;75:1392-1398.
78. Solomon AJ, Watts R, Ontaneda D, Absinta M, Sati P, Reich DS. Diagnostic performance of central vein sign for multiple sclerosis with a simplified three-lesion algorithm. Mult Scler 2017:1352458517726383.
79. Solomon AJ, Naismith RT, Cross AH. Misdiagnosis of multiple sclerosis: Impact of the 2017 McDonald criteria on clinical practice. Neurology 2019;92:26-33.
80. Fisniku LK, Brex PA, Altmann DR, et al. Disability and T2 MRI lesions: a 20-year follow-up of patients with relapse onset of multiple sclerosis. Brain 2008;131:808-817.

81. Tintore M, Rovira A, Rio J, et al. Defining high, medium and low impact prognostic factors for developing multiple sclerosis. Brain 2015;138:1863-1874.
82. Minneboo A, Barkhof F, Polman CH, Uitdehaag BM, Knol DL, Castelijns JA. Infratentorial lesions predict long-term disability in patients with initial findings suggestive of multiple sclerosis. Arch Neurol 2004;61:217-221.
83. Tintore M, Rovira A, Arrambide G, et al. Brainstem lesions in clinically isolated syndromes. Neurology 2010;75:1933-1938.
84. Brownlee WJ, Altmann DR, Alves Da Mota P, et al. Association of asymptomatic spinal cord lesions and atrophy with disability 5 years after a clinically isolated syndrome. Mult Scler 2017;23:665-674.
85. Arrambide G, Rovira A, Sastre-Garriga J, et al. Spinal cord lesions: A modest contributor to diagnosis in clinically isolated syndromes but a relevant prognostic factor. Mult Scler 2018;24:301-312.
86. Brownlee WJ, Altmann DR, Prados F, et al. Early imaging predictors of long-term outcomes in relapse-onset multiple sclerosis. Brain : a journal of neurology 2019;142:2276-2287.
87. Comabella M, Montalban X. Body fluid biomarkers in multiple sclerosis. Lancet Neurol 2014;13:113-126.
88. Khalil M, Teunissen CE, Otto M, et al. Neurofilaments as biomarkers in neurological disorders. Nature reviews Neurology 2018;14:577-589.
89. Petzold A, Balcer LJ, Calabresi PA, et al. Retinal layer segmentation in multiple sclerosis: a systematic review and meta-analysis. Lancet Neurol 2017;16:797-812.
90. Oertel FC, Zimmermann HG, Brandt AU, Paul F. Novel uses of retinal imaging with optical coherence tomography in multiple sclerosis. Expert Rev Neurother 2019;19:31-43.
91. Gabilondo I, Martinez-Lapiscina EH, Fraga-Pumar E, et al. Dynamics of retinal injury after acute optic neuritis. Ann Neurol 2015;77:517-528.
92. Giovannoni G, Tomic D, Bright JR, Havrdova E. "No evident disease activity": The use of combined assessments in the management of patients with multiple sclerosis. Mult Scler 2017;23:1179-1187.
93. Thompson AJ, Miller DH, MacManus DG, McDonald WI. Patterns of disease activity in multiple sclerosis. BMJ 1990;301:44-45.

94. Goodin DS. Magnetic resonance imaging as a surrogate outcome measure of disability in multiple sclerosis: have we been overly harsh in our assessment? Ann Neurol 2006;59:597-605.
95. Li DK, Held U, Petkau J, et al. MRI T2 lesion burden in multiple sclerosis: a plateauing relationship with clinical disability. Neurology 2006;66:1384-1389.
96. Kermode AG, Thompson AJ, Tofts P, et al. Breakdown of the blood-brain barrier precedes symptoms and other MRI signs of new lesions in multiple sclerosis. Pathogenetic and clinical implications. Brain 1990;113 (Pt 5):1477-1489.
97. Thompson AJ, Miller D, Youl B, et al. Serial gadolinium-enhanced MRI in relapsing/remitting multiple sclerosis of varying disease duration. Neurology 1992;42:60-63.
98. Thompson AJ, Kermode AG, Wicks D, et al. Major differences in the dynamics of primary and secondary progressive multiple sclerosis. Ann Neurol 1991;29:53-62.
99. Filippi M, Rossi P, Campi A, Colombo B, Pereira C, Comi G. Serial contrast-enhanced MR in patients with multiple sclerosis and varying levels of disability. AJNR Am J Neuroradiol 1997;18:1549-1556.
100. Swanton JK, Fernando KT, Dalton CM, et al. Early MRI in optic neuritis: the risk for disability. Neurology 2009;72:542-550.
101. Di Filippo M, Anderson VM, Altmann DR, et al. Brain atrophy and lesion load measures over 1 year relate to clinical status after 6 years in patients with clinically isolated syndromes. J Neurol Neurosurg Psychiatry 2010;81:204-208.
102. Absinta M, Sati P, Gaitan MI, et al. Seven-tesla phase imaging of acute multiple sclerosis lesions: a new window into the inflammatory process. Ann Neurol 2013;74:669-678.
103. Gaitan MI, Sati P, Inati SJ, Reich DS. Initial investigation of the blood-brain barrier in MS lesions at 7 tesla. Mult Scler 2013;19:1068-1073.
104. Gaitan MI, Shea CD, Evangelou IE, et al. Evolution of the blood-brain barrier in newly forming multiple sclerosis lesions. Ann Neurol 2011;70:22-29.
105. van Waesberghe JH, van Walderveen MA, Castelijns JA, et al. Patterns of lesion development in multiple sclerosis: longitudinal observations with T1-weighted spin-echo and magnetization transfer MR. AJNR Am J Neuroradiol 1998;19:675-683.

106. van Walderveen MA, Kamphorst W, Scheltens P, et al. Histopathologic correlate of hypointense lesions on T1-weighted spin-echo MRI in multiple sclerosis. Neurology 1998;50:1282-1288.
107. Filippi M, Rocca MA, Barkhof F, et al. Association between pathological and MRI findings in multiple sclerosis. Lancet Neurology 2012;11:349-360.
108. Rocca MA, Comi G, Filippi M. The Role of T1-Weighted Derived Measures of Neurodegeneration for Assessing Disability Progression in Multiple Sclerosis. Front Neurol 2017;8:433.
109. Kuhlmann T, Ludwin S, Prat A, Antel J, Bruck W, Lassmann H. An updated histological classification system for multiple sclerosis lesions. Acta Neuropathol 2017;133:13-24.
110. Bian W, Harter K, Hammond-Rosenbluth KE, et al. A serial in vivo 7T magnetic resonance phase imaging study of white matter lesions in multiple sclerosis. Mult Scler 2013;19:69-75.
111. Chawla S, Kister I, Sinnecker T, et al. Longitudinal study of multiple sclerosis lesions using ultra-high field (7T) multiparametric MR imaging. PLoS One 2018;13:e0202918.
112. Absinta M, Sati P, Schindler M, et al. Persistent 7-tesla phase rim predicts poor outcome in new multiple sclerosis patient lesions. J Clin Invest 2016;126:2597-2609.
113. Absinta M, Sati P, Reich DS. Advanced MRI and staging of multiple sclerosis lesions. Nat Rev Neurol 2016;12:358-368.
114. Chen W, Gauthier SA, Gupta A, et al. Quantitative susceptibility mapping of multiple sclerosis lesions at various ages. Radiology 2014;271:183-192.
115. Sethi V, Nair G, Absinta M, et al. Slowly eroding lesions in multiple sclerosis. Mult Scler 2017;23:464-472.
116. Elliott C, Wolinsky JS, Hauser SL, et al. Slowly expanding/evolving lesions as a magnetic resonance imaging marker of chronic active multiple sclerosis lesions. Mult Scler 2018:1352458518814117.
117. Sinnecker T, Dorr J, Pfueller CF, et al. Distinct lesion morphology at 7-T MRI differentiates neuromyelitis optica from multiple sclerosis. Neurology 2012;79:708-714.

118. Chawla S, Kister I, Wuerfel J, et al. Iron and Non-Iron-Related Characteristics of Multiple Sclerosis and Neuromyelitis Optica Lesions at 7T MRI. AJNR Am J Neuroradiol 2016;37:1223-1230.
119. Kilsdonk ID, Lopez-Soriano A, Kuijer JP, et al. Morphological features of MS lesions on FLAIR* at 7 T and their relation to patient characteristics. J Neurol 2014;261:1356-1364.
120. Rocca MA, Battaglini M, Benedict RH, et al. Brain MRI atrophy quantification in MS: From methods to clinical application. Neurology 2017;88:403-413.
121. Filippi M, Preziosa P, Rocca MA. Microstructural MR Imaging Techniques in Multiple Sclerosis. Neuroimaging Clin N Am 2017;27:313-333.
122. Schmierer K, Wheeler-Kingshott CA, Boulby PA, et al. Diffusion tensor imaging of post mortem multiple sclerosis brain. Neuroimage 2007;35:467-477.
123. Vavasour IM, Laule C, Li DK, Traboulsee AL, MacKay AL. Is the magnetization transfer ratio a marker for myelin in multiple sclerosis? J Magn Reson Imaging 2011;33:713-718.
124. Schmierer K, Scaravilli F, Altmann DR, Barker GJ, Miller DH. Magnetization transfer ratio and myelin in postmortem multiple sclerosis brain. Ann Neurol 2004;56:407-415.
125. Filippi M, Rocca MA, Ciccarelli O, et al. MRI criteria for the diagnosis of multiple sclerosis: MAGNIMS consensus guidelines. Lancet Neurol 2016;15:292-303.
126. Filippi M, Preziosa P, Meani A, et al. Prediction of a multiple sclerosis diagnosis in patients with clinically isolated syndrome using the 2016 MAGNIMS and 2010 McDonald criteria: a retrospective study. Lancet Neurol 2018;17:133-142.
127. Sati P, Oh J, Constable RT, et al. The central vein sign and its clinical evaluation for the diagnosis of multiple sclerosis: a consensus statement from the North American Imaging in Multiple Sclerosis Cooperative. Nat Rev Neurol 2016;12:714-722.
128. Sinnecker T, Clarke MA, Meier D, et al. Evaluation of the Central Vein Sign as a Diagnostic Imaging Biomarker in Multiple Sclerosis. JAMA Neurol 2019.
129. Kister I, Herbert J, Zhou Y, Ge Y. Ultrahigh-Field MR (7 T) Imaging of Brain Lesions in Neuromyelitis Optica. Mult Scler Int 2013;2013:398259.

130. Maggi P, Absinta M, Grammatico M, et al. Central vein sign differentiates Multiple Sclerosis from central nervous system inflammatory vasculopathies. Ann Neurol 2018;83:283-294.
131. Solomon AJ, Schindler MK, Howard DB, et al. "Central vessel sign" on 3T FLAIR* MRI for the differentiation of multiple sclerosis from migraine. Ann Clin Transl Neurol 2016;3:82-87.
132. Wuerfel J, Sinnecker T, Ringelstein EB, et al. Lesion morphology at 7 Tesla MRI differentiates Susac syndrome from multiple sclerosis. Mult Scler 2012;18:1592-1599.
133. Campion T, Smith RJP, Altmann DR, et al. FLAIR* to visualize veins in white matter lesions: A new tool for the diagnosis of multiple sclerosis? Eur Radiol 2017;27:4257-4263.
134. Mistry N, Abdel-Fahim R, Samaraweera A, et al. Imaging central veins in brain lesions with 3-T T2*-weighted magnetic resonance imaging differentiates multiple sclerosis from microangiopathic brain lesions. Mult Scler 2016;22:1289-1296.
135. Samaraweera AP, Clarke MA, Whitehead A, et al. The Central Vein Sign in Multiple Sclerosis Lesions Is Present Irrespective of the T2* Sequence at 3 T. J Neuroimaging 2017;27:114-121.
136. Tallantyre EC, Dixon JE, Donaldson I, et al. Ultra-high-field imaging distinguishes MS lesions from asymptomatic white matter lesions. Neurology 2011;76:534-539.
137. Glasser MF, Van Essen DC. Mapping human cortical areas in vivo based on myelin content as revealed by T1- and T2-weighted MRI. J Neurosci 2011;31:11597-11616.
138. Clark VP, Courchesne E, Grafe M. In vivo myeloarchitectonic analysis of human striate and extrastriate cortex using magnetic resonance imaging. Cereb Cortex 1992;2:417-424.
139. Yoshiura T, Higano S, Rubio A, et al. Heschl and superior temporal gyri: low signal intensity of the cortex on T2-weighted MR images of the normal brain. Radiology 2000;214:217-221.
140. Koenig SH. Cholesterol of myelin is the determinant of gray-white contrast in MRI of brain. Magn Reson Med 1991;20:285-291.

141. Miot-Noirault E, Barantin L, Akoka S, Le Pape A. T2 relaxation time as a marker of brain myelination: experimental MR study in two neonatal animal models. J Neurosci Methods 1997;72:5-14.
142. Fukunaga M, Li TQ, van Gelderen P, et al. Layer-specific variation of iron content in cerebral cortex as a source of MRI contrast. Proc Natl Acad Sci U S A 2010;107:3834-3839.
143. Glasser MF, Coalson TS, Robinson EC, et al. A multi-modal parcellation of human cerebral cortex. Nature 2016;536:171-178.
144. Pareto D, Garcia-Vidal A, Alberich M, et al. Ratio of T1-Weighted to T2-Weighted Signal Intensity as a Measure of Tissue Integrity: Comparison with Magnetization Transfer Ratio in Patients with Multiple Sclerosis. AJNR Am J Neuroradiol 2020;41:461-463.
145. Nakamura K, Chen JT, Ontaneda D, Fox RJ, Trapp BD. T1-/T2-weighted ratio differs in demyelinated cortex in multiple sclerosis. Ann Neurol 2017;82:635-639.
146. Uddin MN, Figley TD, Solar KG, Shatil AS, Figley CR. Comparisons between multi-component myelin water fraction, T1w/T2w ratio, and diffusion tensor imaging measures in healthy human brain structures. Sci Rep 2019;9:2500.
147. Natu VS, Gomez J, Barnett M, et al. Apparent thinning of human visual cortex during childhood is associated with myelination. Proc Natl Acad Sci U S A 2019;116:20750-20759.
148. Righart R, Biberacher V, Jonkman LE, et al. Cortical pathology in multiple sclerosis detected by the T1/T2-weighted ratio from routine magnetic resonance imaging. Ann Neurol 2017;82:519-529.
149. Rocca MA, Valsasina P, Meani A, et al. Association of Gray Matter Atrophy Patterns With Clinical Phenotype and Progression in Multiple Sclerosis. Neurology 2021;96:e1561-e1573.
150. Zheng Y, Dudman J, Chen JT, et al. Sensitivity of T1/T2-weighted ratio in detection of cortical demyelination is similar to magnetization transfer ratio using post-mortem MRI. Mult Scler 2021:13524585211014760.
151. Pelkmans W, Dicks E, Barkhof F, et al. Gray matter T1-w/T2-w ratios are higher in Alzheimer's disease. Hum Brain Mapp 2019;40:3900-3909.

152. Du G, Lewis MM, Sica C, Kong L, Huang X. Magnetic resonance T1w/T2w ratio: A parsimonious marker for Parkinson disease. Ann Neurol 2019;85:96-104.
153. Preziosa P, Bouman PM, Kiljan S, et al. Neurite density explains cortical T1-weighted/T2-weighted ratio in multiple sclerosis. J Neurol Neurosurg Psychiatry 2021;92:790-792.
154. Nerland S, Jorgensen KN, Nordhoy W, et al. Multisite reproducibility and test-retest reliability of the T1w/T2w-ratio: A comparison of processing methods. Neuroimage 2021:118709.
155. Collins CM, Smith MB. Signal-to-noise ratio and absorbed power as functions of main magnetic field strength, and definition of "90 degrees " RF pulse for the head in the birdcage coil. Magn Reson Med 2001;45:684-691.
156. Lutti A, Hutton C, Finsterbusch J, Helms G, Weiskopf N. Optimization and validation of methods for mapping of the radiofrequency transmit field at 3T. Magn Reson Med 2010;64:229-238.
157. Ganzetti M, Wenderoth N, Mantini D. Whole brain myelin mapping using T1- and T2-weighted MR imaging data. Front Hum Neurosci 2014;8:671.
158. Misaki M, Savitz J, Zotev V, et al. Contrast enhancement by combining T1- and T2-weighted structural brain MR Images. Magn Reson Med 2015;74:1609-1620.
159. Cacciaguerra L, Rocca MA, Storelli L, Radaelli M, Filippi M. Mapping white matter damage distribution in neuromyelitis optica spectrum disorders with a multimodal MRI approach. Mult Scler 2021;27:841-854.
160. Beer A, Biberacher V, Schmidt P, et al. Tissue damage within normal appearing white matter in early multiple sclerosis: assessment by the ratio of T1- and T2-weighted MR image intensity. J Neurol 2016;263:1495-1502.
161. Cooper G, Chien C, Zimmermann H, et al. Longitudinal analysis of T1w/T2w ratio in patients with multiple sclerosis from first clinical presentation. Mult Scler 2021:13524585211003479.
162. Cooper G, Finke C, Chien C, et al. Standardization of T1w/T2w Ratio Improves Detection of Tissue Damage in Multiple Sclerosis. Front Neurol 2019;10:334.
163. Preziosa P, Storelli L, Meani A, et al. Effects of Fingolimod and Natalizumab on Brain T1-/T2-Weighted and Magnetization Transfer Ratios: a 2-Year Study. Neurotherapeutics 2021;18:878-888.

164. Granberg T, Fan Q, Treaba CA, et al. In vivo characterization of cortical and white matter neuroaxonal pathology in early multiple sclerosis. Brain 2017;140:2912-2926.
165. Petracca M, El Mendili MM, Moro M, et al. Laminar analysis of the cortical T1/T2-weighted ratio at 7T. Neurol Neuroimmunol Neuroinflamm 2020;7.
166. Eshaghi A, Young AL, Wijeratne PA, et al. Identifying multiple sclerosis subtypes using unsupervised machine learning and MRI data. Nat Commun 2021;12:2078.
167. Kurtzke JF. Rating neurologic impairment in multiple sclerosis: an expanded disability status scale (EDSS). Neurology 1983;33:1444-1452.
168. Valverde S, Cabezas M, Roura E, et al. Improving automated multiple sclerosis lesion segmentation with a cascaded 3D convolutional neural network approach. Neuroimage 2017;155:159-168.
169. Smith SM, De Stefano N, Jenkinson M, Matthews PM. Normalized accurate measurement of longitudinal brain change. J Comput Assist Tomogr 2001;25:466-475.
170. Battaglini M, Jenkinson M, De Stefano N. Evaluating and reducing the impact of white matter lesions on brain volume measurements. Hum Brain Mapp 2012;33:2062-2071.
171. Chard DT, Jackson JS, Miller DH, Wheeler-Kingshott CA. Reducing the impact of white matter lesions on automated measures of brain gray and white matter volumes. J Magn Reson Imaging 2010;32:223-228.
172. Patenaude B, Smith SM, Kennedy DN, Jenkinson M. A Bayesian model of shape and appearance for subcortical brain segmentation. Neuroimage 2011;56:907-922.
173. Damjanovic D, Valsasina P, Rocca MA, et al. Hippocampal and Deep Gray Matter Nuclei Atrophy Is Relevant for Explaining Cognitive Impairment in MS: A Multicenter Study. AJNR Am J Neuroradiol 2017;38:18-24.
174. Schoonheim MM, Popescu V, Rueda Lopes FC, et al. Subcortical atrophy and cognition: sex effects in multiple sclerosis. Neurology 2012;79:1754-1761.
175. Tustison NJ, Avants BB, Cook PA, et al. N4ITK: improved N3 bias correction. IEEE Trans Med Imaging 2010;29:1310-1320.
176. Grydeland H, Walhovd KB, Tamnes CK, Westlye LT, Fjell AM. Intracortical myelin links with performance variability across the human lifespan: results from

T1- and T2-weighted MRI myelin mapping and diffusion tensor imaging. J Neurosci 2013;33:18618-18630.

177. Tullo S, Patel R, Devenyi GA, et al. MR-based age-related effects on the striatum, globus pallidus, and thalamus in healthy individuals across the adult lifespan. Hum Brain Mapp 2019;40:5269-5288.
178. Yeatman JD, Wandell BA, Mezer AA. Lifespan maturation and degeneration of human brain white matter. Nat Commun 2014;5:4932.
179. Emery B. Regulation of oligodendrocyte differentiation and myelination. Science 2010;330:779-782.
180. Benes FM. Myelination of cortical-hippocampal relays during late adolescence. Schizophr Bull 1989;15:585-593.
181. Benes FM, Turtle M, Khan Y, Farol P. Myelination of a key relay zone in the hippocampal formation occurs in the human brain during childhood, adolescence, and adulthood. Arch Gen Psychiatry 1994;51:477-484.
182. Moller HE, Bossoni L, Connor JR, et al. Iron, Myelin, and the Brain: Neuroimaging Meets Neurobiology. Trends Neurosci 2019;42:384-401.
183. Todorich B, Pasquini JM, Garcia CI, Paez PM, Connor JR. Oligodendrocytes and myelination: the role of iron. Glia 2009;57:467-478.
184. Boxerman JL, Hamberg LM, Rosen BR, Weisskoff RM. MR contrast due to intravascular magnetic susceptibility perturbations. Magn Reson Med 1995;34:555-566.
185. Gossuin Y, Gillis P, Muller RN, Hocq A. Relaxation by clustered ferritin: a model for ferritin-induced relaxation in vivo. NMR Biomed 2007;20:749-756.
186. Zivadinov R, Tavazzi E, Bergsland N, et al. Brain Iron at Quantitative MRI Is Associated with Disability in Multiple Sclerosis. Radiology 2018;289:487-496.
187. Drayer B, Burger P, Darwin R, Riederer S, Herfkens R, Johnson GA. MRI of brain iron. AJR Am J Roentgenol 1986;147:103-110.
188. Hallgren B, Sourander P. The effect of age on the non-haemin iron in the human brain. J Neurochem 1958;3:41-51.
189. Milton WJ, Atlas SW, Lexa FJ, Mozley PD, Gur RE. Deep gray matter hypointensity patterns with aging in healthy adults: MR imaging at 1.5 T. Radiology 1991;181:715-719.

190. Connor JR, Menzies SL, St Martin SM, Mufson EJ. Cellular distribution of transferrin, ferritin, and iron in normal and aged human brains. J Neurosci Res 1990;27:595-611.
191. Zhang X, Surguladze N, Slagle-Webb B, Cozzi A, Connor JR. Cellular iron status influences the functional relationship between microglia and oligodendrocytes. Glia 2006;54:795-804.
192. Hametner S, Endmayr V, Deistung A, et al. The influence of brain iron and myelin on magnetic susceptibility and effective transverse relaxation - A biochemical and histological validation study. Neuroimage 2018;179:117-133.
193. Aquino D, Bizzi A, Grisoli M, et al. Age-related iron deposition in the basal ganglia: quantitative analysis in healthy subjects. Radiology 2009;252:165-172.
194. Langkammer C, Liu T, Khalil M, et al. Quantitative susceptibility mapping in multiple sclerosis. Radiology 2013;267:551-559.
195. Zhang Y, Wei H, Cronin MJ, He N, Yan F, Liu C. Longitudinal atlas for normative human brain development and aging over the lifespan using quantitative susceptibility mapping. Neuroimage 2018;171:176-189.
196. Hametner S, Wimmer I, Haider L, Pfeifenbring S, Bruck W, Lassmann H. Iron and neurodegeneration in the multiple sclerosis brain. Ann Neurol 2013;74:848-861.
197. Castriota Scanderbeg A, Tomaiuolo F, Sabatini U, Nocentini U, Grasso MG, Caltagirone C. Demyelinating plaques in relapsing-remitting and secondary-progressive multiple sclerosis: assessment with diffusion MR imaging. AJNR Am J Neuroradiol 2000;21:862-868.
198. Rocca MA, Mastronardo G, Rodegher M, Comi G, Filippi M. Long-term changes of magnetization transfer-derived measures from patients with relapsing-remitting and secondary progressive multiple sclerosis. AJNR Am J Neuroradiol 1999;20:821-827.
199. Preziosa P, Rocca MA, Mesaros S, et al. Intrinsic damage to the major white matter tracts in patients with different clinical phenotypes of multiple sclerosis: a voxelwise diffusion-tensor MR study. Radiology 2011;260:541-550.
200. Griffin CM, Chard DT, Ciccarelli O, et al. Diffusion tensor imaging in early relapsing-remitting multiple sclerosis. Mult Scler 2001;7:290-297.

201. Filippi M, Rocca MA, Martino G, Horsfield MA, Comi G. Magnetization transfer changes in the normal appearing white matter precede the appearance of enhancing lesions in patients with multiple sclerosis. Ann Neurol 1998;43:809-814.
202. Audoin B, Davies G, Rashid W, Fisniku L, Thompson AJ, Miller DH. Voxel-based analysis of grey matter magnetization transfer ratio maps in early relapsing remitting multiple sclerosis. Mult Scler 2007;13:483-489.
203. Crespy L, Zaaraoui W, Lemaire M, et al. Prevalence of grey matter pathology in early multiple sclerosis assessed by magnetization transfer ratio imaging. PLoS One 2011;6:e24969.
204. Audoin B, Ranjeva JP, Au Duong MV, et al. Voxel-based analysis of MTR images: a method to locate gray matter abnormalities in patients at the earliest stage of multiple sclerosis. J Magn Reson Imaging 2004;20:765-771.
205. Filippi M, Preziosa P, Copetti M, et al. Gray matter damage predicts the accumulation of disability 13 years later in MS. Neurology 2013;81:1759-1767.
206. Haider L, Prados F, Chung K, et al. Cortical involvement determines impairment 30 years after a clinically isolated syndrome. Brain 2021;144:1384-1395.
207. Bartzokis G, Tishler TA, Lu PH, et al. Brain ferritin iron may influence age- and gender-related risks of neurodegeneration. Neurobiol Aging 2007;28:414-423.
208. Rowley CD, Tabrizi SJ, Scahill RI, et al. Altered Intracortical T1-Weighted/T2-Weighted Ratio Signal in Huntington's Disease. Front Neurosci 2018;12:805.
209. Sugiyama A, Cooper G, Hirano S, et al. Cognitive Impairment in Multiple System Atrophy Is Related to White Matter Damage Detected by the T1-Weighted/T2-Weighted Ratio. Eur Neurol 2021:1-9.
210. Cifelli A, Arridge M, Jezzard P, Esiri MM, Palace J, Matthews PM. Thalamic neurodegeneration in multiple sclerosis. Ann Neurol 2002;52:650-653.
211. Haider L, Simeonidou C, Steinberger G, et al. Multiple sclerosis deep grey matter: the relation between demyelination, neurodegeneration, inflammation and iron. J Neurol Neurosurg Psychiatry 2014;85:1386-1395.
212. Vercellino M, Masera S, Lorenzatti M, et al. Demyelination, inflammation, and neurodegeneration in multiple sclerosis deep gray matter. J Neuropathol Exp Neurol 2009;68:489-502.

213. Pontillo G, Petracca M, Monti S, et al. Unraveling Deep Gray Matter Atrophy and Iron and Myelin Changes in Multiple Sclerosis. AJNR Am J Neuroradiol 2021;42:1223-1230.
214. Burgetova A, Dusek P, Vaneckova M, et al. Thalamic Iron Differentiates Primary-Progressive and Relapsing-Remitting Multiple Sclerosis. AJNR Am J Neuroradiol 2017;38:1079-1086.